

e+BOOST  
PRIN2022-  
2022Y87K7X

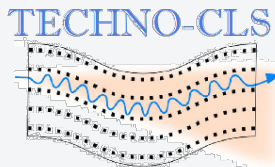
Ministero  
dell'Università  
e della Ricerca  
**Bando  
PRIN 2022**  
UNIVERSITÀ RICERCA

Finanziato  
dall'Unione europea  
NextGenerationEU

Ministero  
dell'Università  
e della Ricerca

Italiadomani  
PIANO NAZIONALE  
DI RIPRESA E RESILIENZA

INFN  
FERRARA



EIC-PATHFINDER-OPEN  
TECHNO-CLS  
(GA 101046458)

UC Lab  
Irène Joliot-Curie  
Laboratoire de Physique  
des 2 Infinis

anr  
GA No ANR-21-CE31-0007



# Experiments on crystal radiators at DESY and CERN PS TB

2<sup>nd</sup> FCC-France&Italy workshop – Venice



**Nicola Canale**

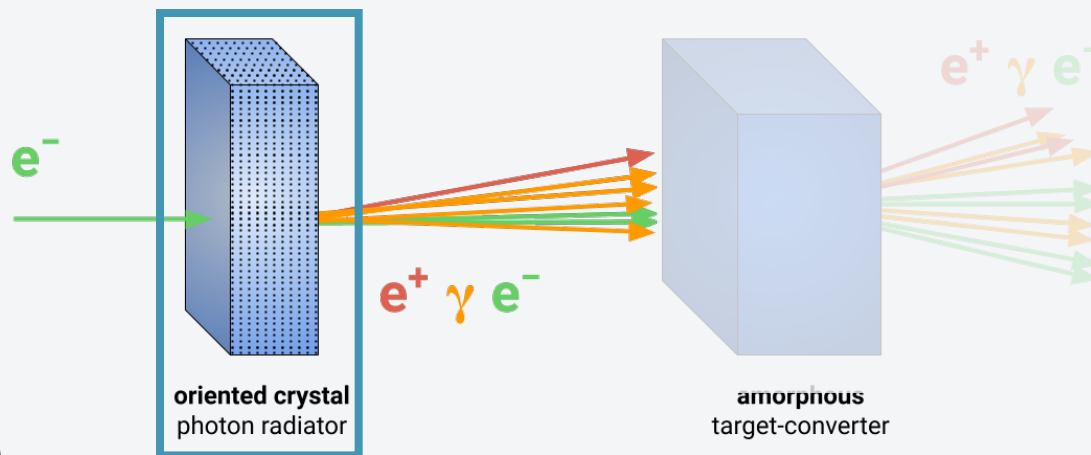
on behalf of F. Alharthi, A. Bacci, L. Bandiera, D. Boccanfuso, S. Carsi, I. Chaikovska, R. Chehab, D. De Salvador, P. Fedeli, V. Guidi, V. Haurylavets, O. Iorio, G. Lezzani, L. Malagutti, S. Mangiacavalli, A. Mazzolari, P. Monti Guarnieri, V. Mytrochenko, R. Negrello, G. Paternò, M. Prest, M. Romagnoni, M. Rossetti Conti, A. Selmi, F. Sgarbossa, M. Soldani, A. Sytov, V. Tikhomirov, E. Vallazza

INFN Ferrara  
[ncanale@fe.infn.it](mailto:ncanale@fe.infn.it)

# Outlook

As presented in talks by A. Sytov and G. Paternò, **crystal-based positron sources** offer promising potential for future colliders.

Here, we will see the **test beam results on crystal radiators**, which serve as a crucial **benchmark for simulation code validation**.



# Outlook

As presented in talks by **A. Sytov** and **G. Paternò**, **crystal-based positron sources** offer promising potential for future colliders.

Here, we will see the **test beam results** on **crystal radiators**, which serve as a crucial **benchmark** for **simulation code** validation.

- **THE CRYSTALS**
- **EXPERIMENTAL SETUP**
- **TESTBEAM RESULTS**

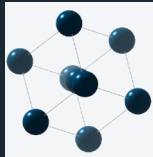
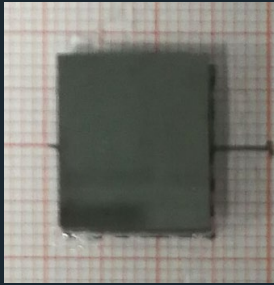




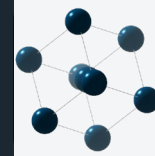
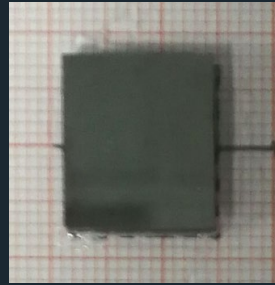
# THE CRYSTALS



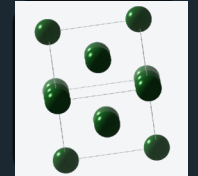
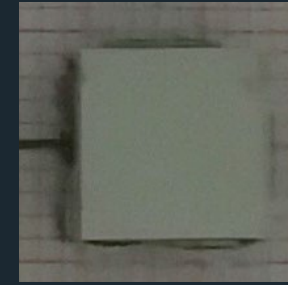
# Crystal radiators



Material: **Tungsten (W)**  
channelling Axis: **<100>**  
 $\theta_C \approx 0.5 \text{ mrad}$   
Thickness: **2.25 mm (0.64 X0)**  
(**research center** manufactured crystal)



Material: **Tungsten (W)**  
channelling Axis: **<111>** (most efficient)  
 $\theta_C \approx 0.6 \text{ mrad}$   
Thickness: **1.5-2 mm (0.43 – 0.57 X0)**  
(**industrially** manufactured crystals)



Material: **Iridium (Ir)**  
channelling Axis: **<110>** (most efficient)  
 $\theta_C \approx 0.6$   
Thickness: **1 -2 mm (0.34 – 0.68 X0)**  
(**industrially** manufactured crystals)

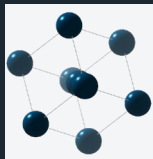
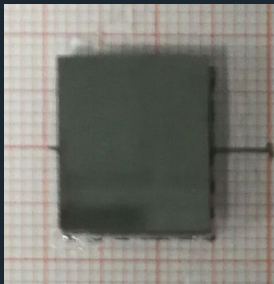
Tested at DESY T21 beamline with 5.6 GeV/c electrons



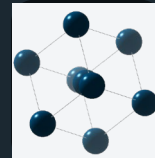
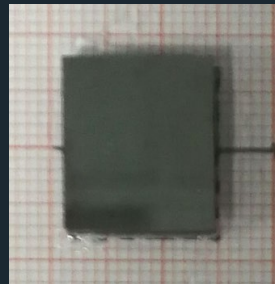
Tested at CERN PS T9 beamline with 6 GeV/c electrons



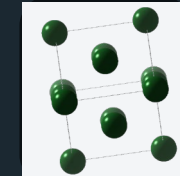
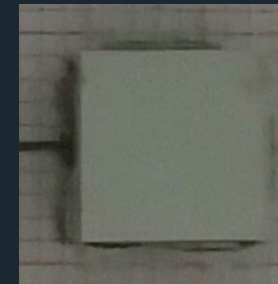
# Crystal radiators



Material: **Tungsten (W)**  
channelling Axis: **<100>**  
 $\theta_C \approx 0.5 \text{ mrad}$   
Thickness: **2.25 mm (0.64 X0)**  
(**research center** manufactured crystal)



Material: **Tungsten (W)**  
channelling Axis: **<111>** (most efficient)  
 $\theta_C \approx 0.6 \text{ mrad}$   
Thickness: **1.5-2 mm (0.43 – 0.57 X0)**  
(**industrially** manufactured crystals)



Material: **Iridium (Ir)**  
channelling Axis: **<110>** (most efficient)  
 $\theta_C \approx 0.6$   
Thickness: **1 -2 mm (0.34 – 0.68 X0)**  
(**industrially** manufactured crystals)

Research Center quality crystal

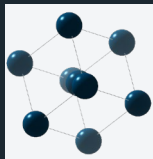
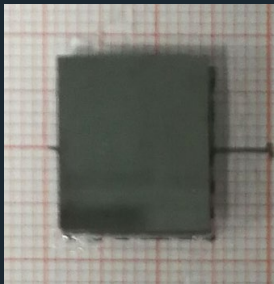
Tested at DESY T21 beamline with 5.6 GeV/c electrons



Tested at CERN PS T9 beamline with 6 GeV/c electrons



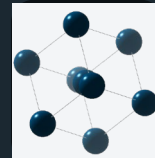
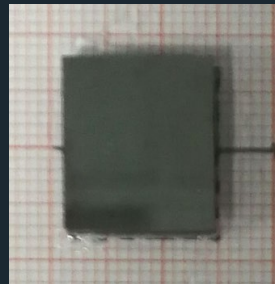
# Crystal radiators



Material: **Tungsten (W)**  
channelling Axis: **<100>**  
 $\theta_C \approx 0.5 \text{ mrad}$   
Thickness: **2.25 mm (0.64 X0)**  
(**research center** manufactured crystal)

Research Center quality crystal

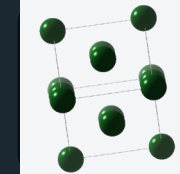
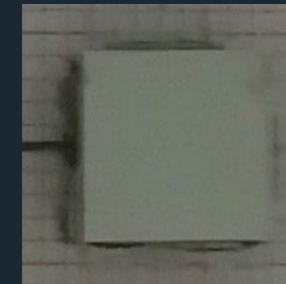
Tested at DESY T21 beamline with 5.6 GeV/c electrons



Material: **Tungsten (W)**  
channelling Axis: **<111>** (most efficient)  
 $\theta_C \approx 0.6 \text{ mrad}$   
Thickness: **1.5-2 mm (0.43 – 0.57 X0)**  
(**industrially** manufactured crystals)

W 2mm baseline for Hybrid source radiator - 1.5mm for optimization studies

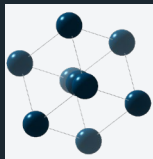
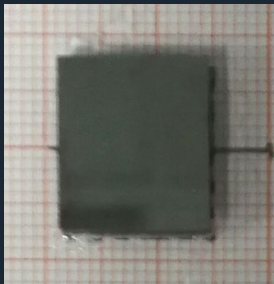
Tested at CERN PS T9 beamline with 6 GeV/c electrons



Material: **Iridium (Ir)**  
channelling Axis: **<110>** (most efficient)  
 $\theta_C \approx 0.6$   
Thickness: **1 -2 mm (0.34 – 0.68 X0)**  
(**industrially** manufactured crystals)



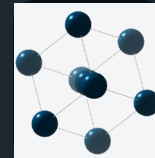
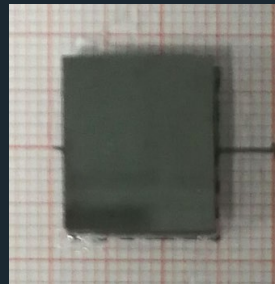
# Crystal radiators



Material: **Tungsten (W)**  
channelling Axis: **<100>**  
 $\theta_C \approx 0.5 \text{ mrad}$   
Thickness: **2.25 mm (0.64 X0)**  
(**research center** manufactured crystal)

Research Center quality crystal

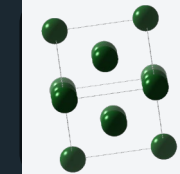
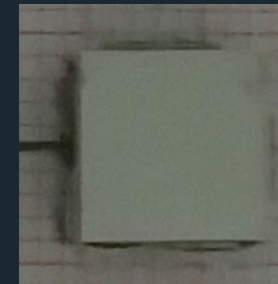
Tested at DESY T21 beamline with 5.6 GeV/c electrons



Material: **Tungsten (W)**  
channelling Axis: **<111>** (most efficient)  
 $\theta_C \approx 0.6 \text{ mrad}$   
Thickness: **1.5-2 mm (0.43 – 0.57 X0)**  
(**industrially** manufactured crystals)

W 2mm baseline for Hybrid source radiator - 1.5mm for optimization studies

Tested at CERN PS T9 beamline with 6 GeV/c electrons



Material: **Iridium (Ir)**  
channelling Axis: **<110>** (most efficient)  
 $\theta_C \approx 0.6$   
Thickness: **1 -2 mm (0.34 – 0.68 X0)**  
(**industrially** manufactured crystals)

Higher potential, interesting alternative



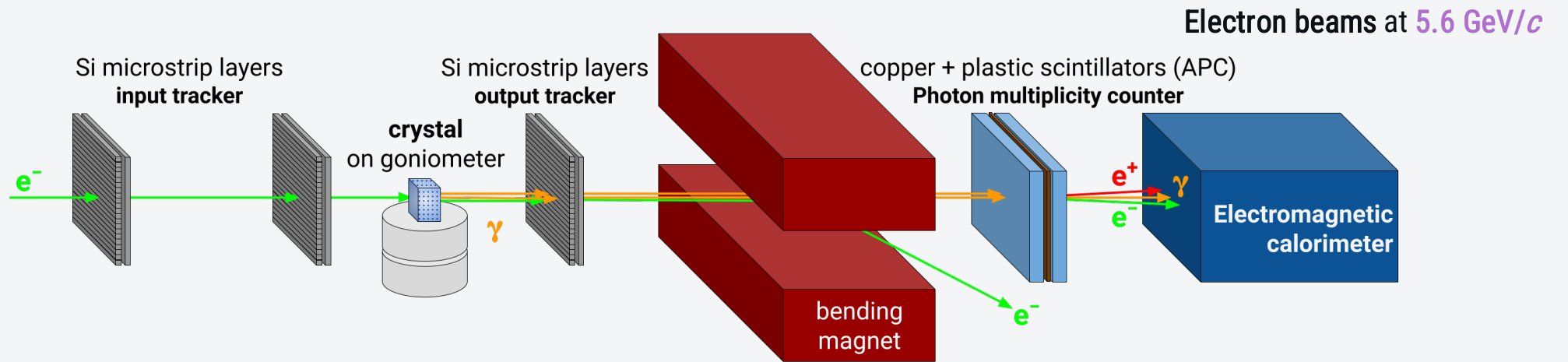


# EXPERIMENTAL SETUP

# The setup



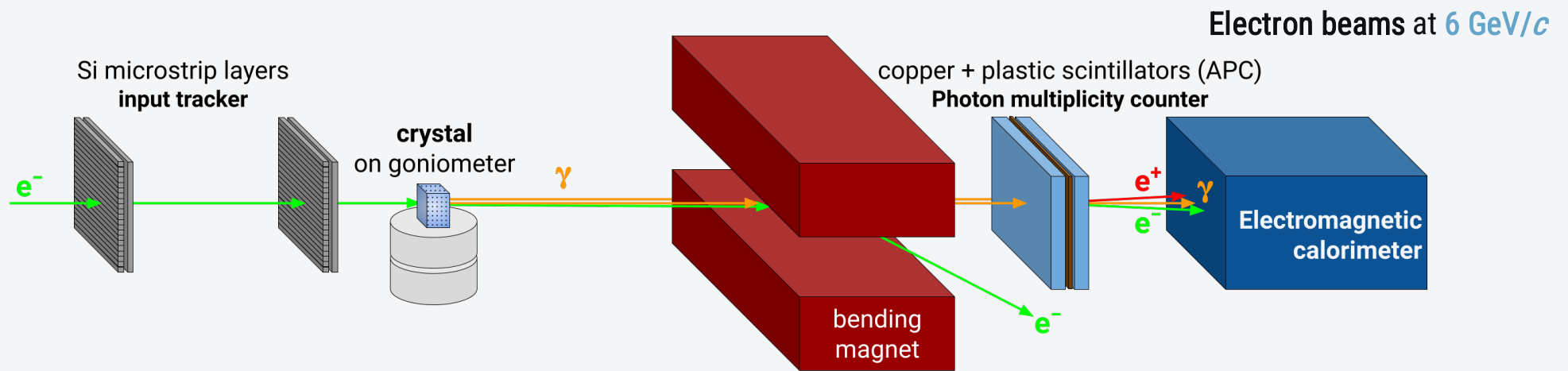
DESY setup configuration



Provided by INFN Milano Bicocca team – Erik Vallazza & Michela Prest



# The setup

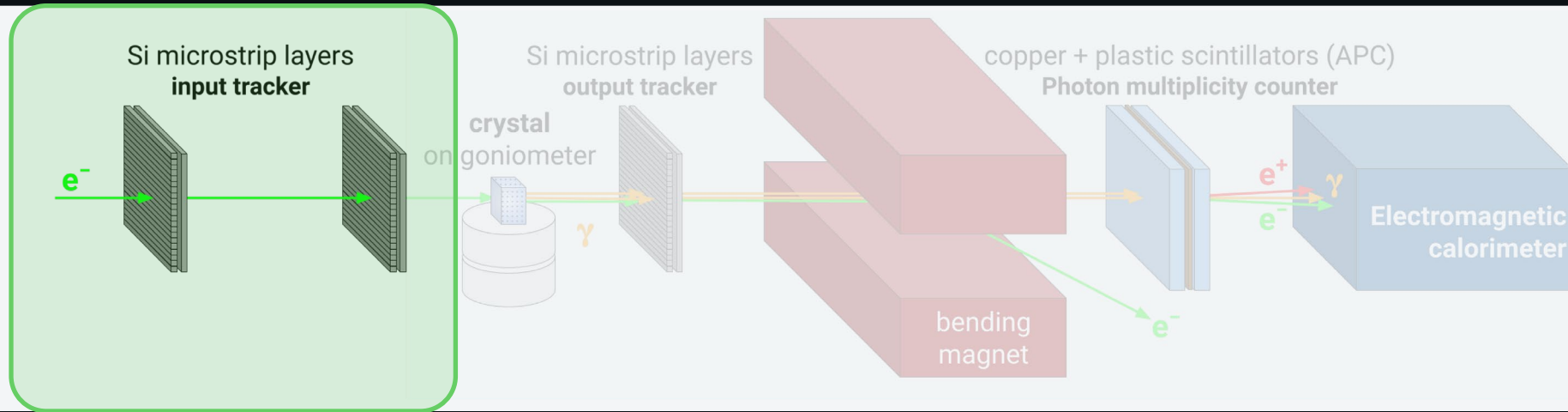


Provided by INFN Milano Bicocca team – Erik Vallazza & Michela Prest

# The setup

CERN  
configuration

DESY  
configuration



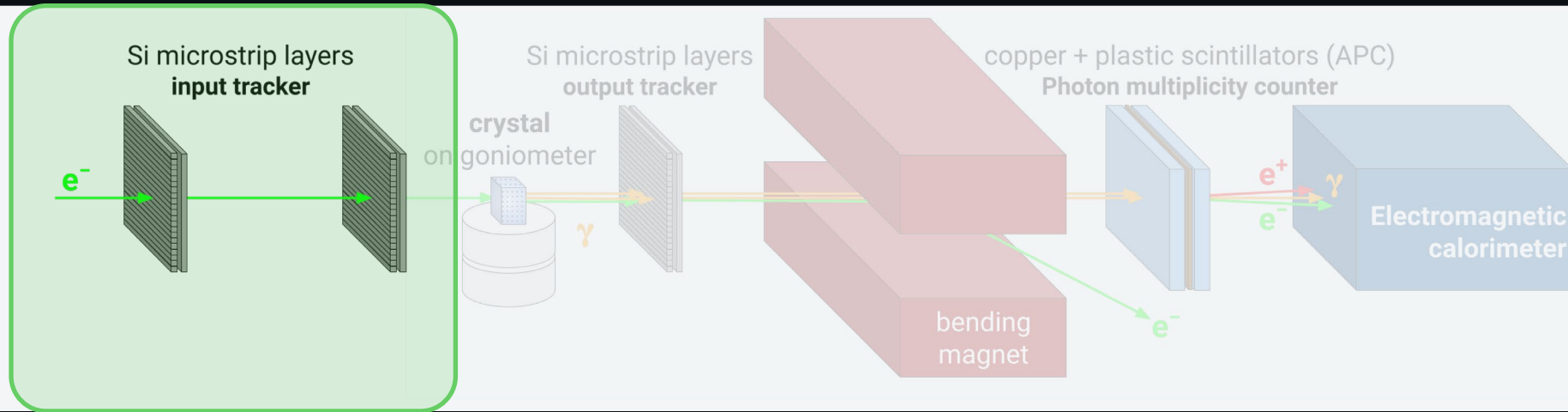
## Input stage

Reconstruct track and  
impinging angle on the  
crystal

# The setup

CERN  
configuration

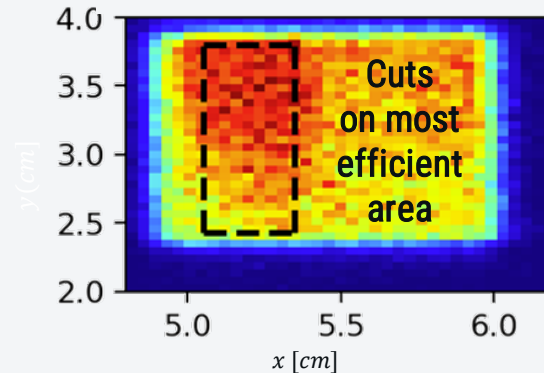
DESY  
configuration



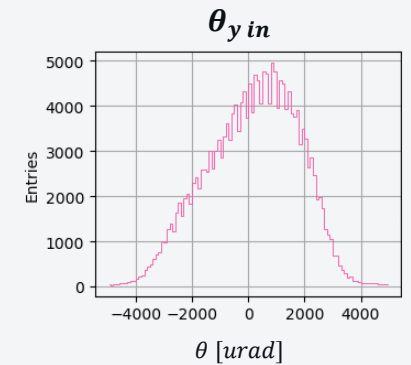
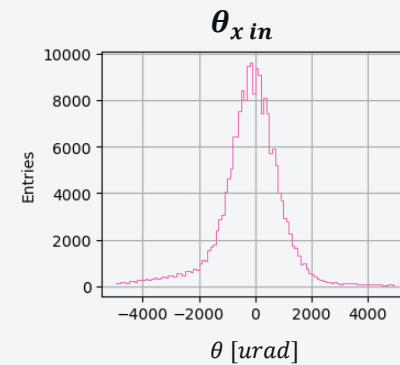
## Input stage

Reconstruct track and impinging angle on the crystal

Crystal reconstructed position



Impinging angles





# The setup - **input stage**

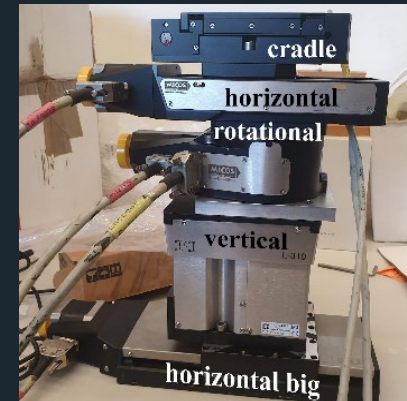
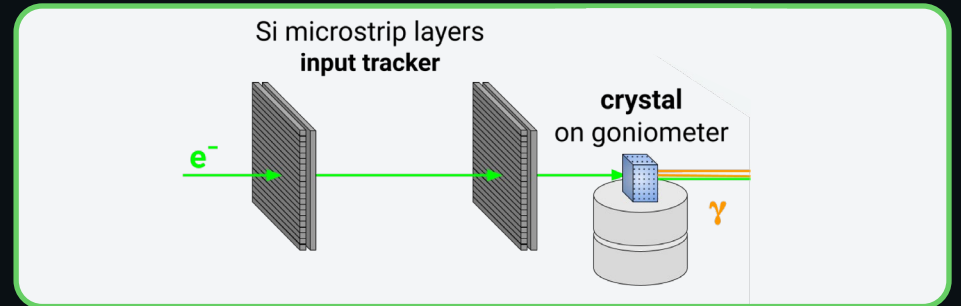
## Input tracker

~  $2 \times 2 \text{ cm}^2$   $xy$  double-sided Si microstrip sensors, with an overall  $\sim 10 \text{ }\mu\text{m}$  single-hit resolution.

~  $9.5 \times 9.5 \text{ cm}^2$   $xy$  double-sided Si microstrip sensors, with an overall  $\sim 40 \text{ }\mu\text{m}$  single-hit resolution.

## Goniometer from LNL & UNIPD

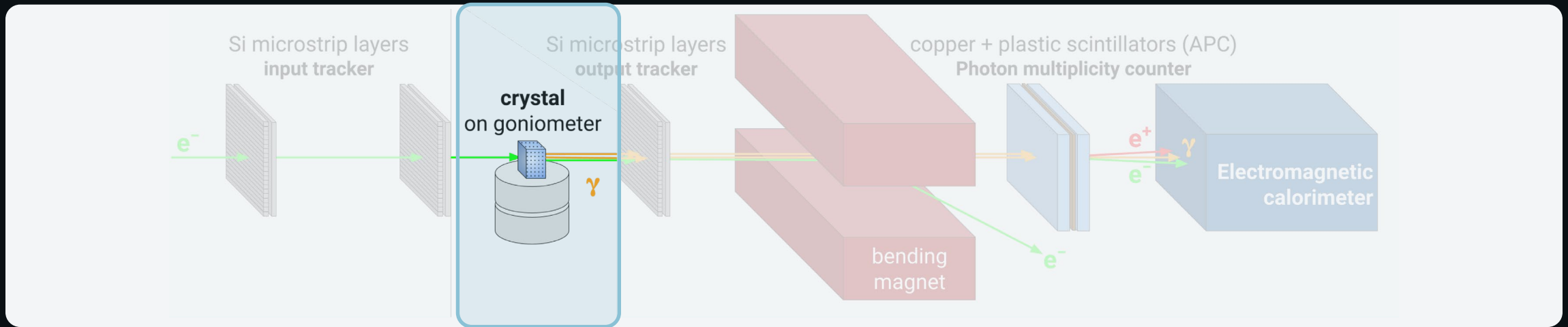
Fine-grained, remote-controlled movements along  $x, y, \theta_x$  and  $\theta_y$  with  $\sim 5 \text{ }\mu\text{m}$ ,  $1 \text{ }\mu\text{rad}$  resolution.



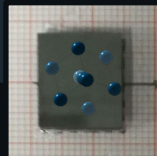
# The setup - the crystal

CERN  
configuration

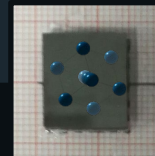
DESY  
configuration



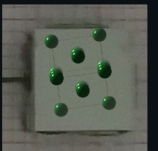
Material: Tungsten (2.25 mm)  
channelling Axis:  $\langle 100 \rangle$   
Axial potential: 1 keV  
 $\theta_c \approx 0.5 \text{ mrad}$



Material: Tungsten (1.5-2 mm)  
channelling Axis:  $\langle 111 \rangle$   
Axial potential: 1 keV  
 $\theta_c \approx 0.6 \text{ mrad}$



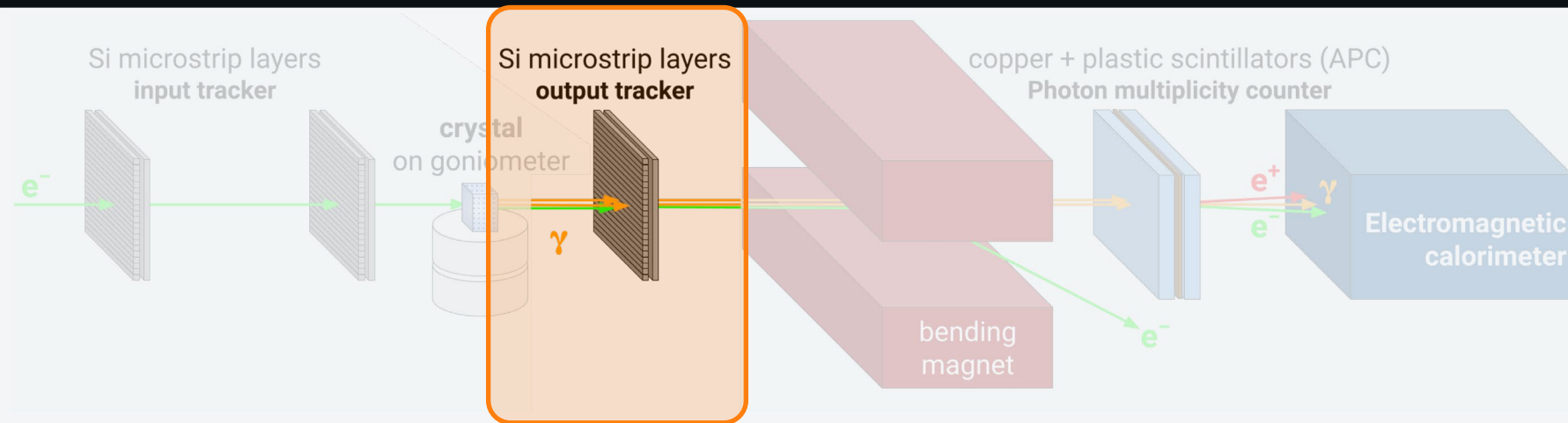
Material: Iridium (1-2 mm)  
channelling Axis:  $\langle 110 \rangle$   
Axial potential: 1 keV  
 $\theta_c \approx 0.6 \text{ mrad}$



# The setup - **output tracker**



DESY setup configuration



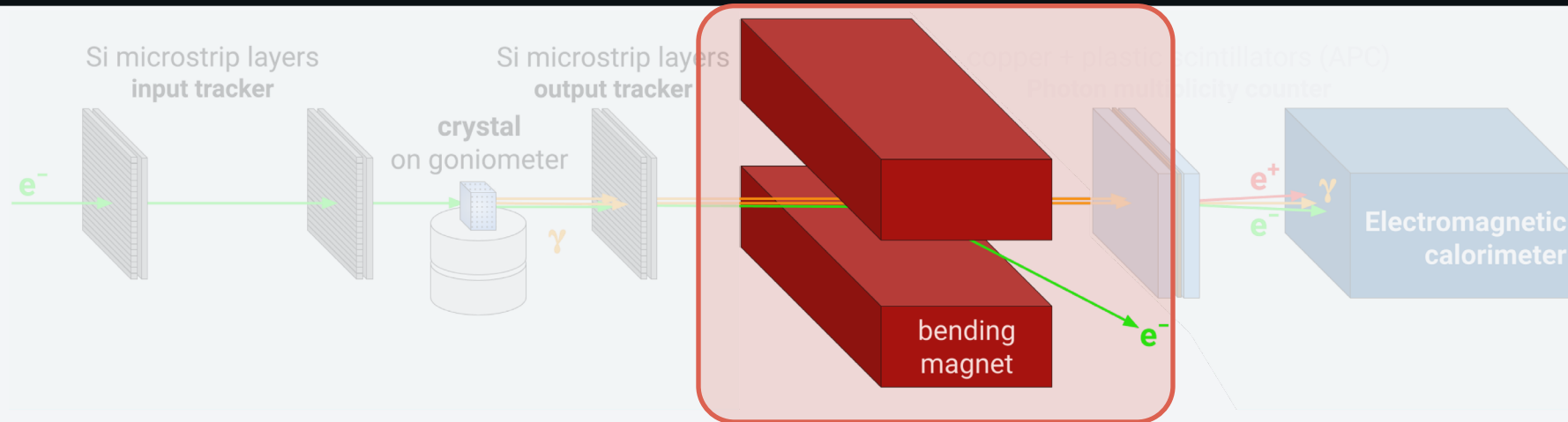
**output tracker**  
As multiplicity counter to align the  
crystal



# The setup - magnet

CERN  
configuration

DESY  
configuration

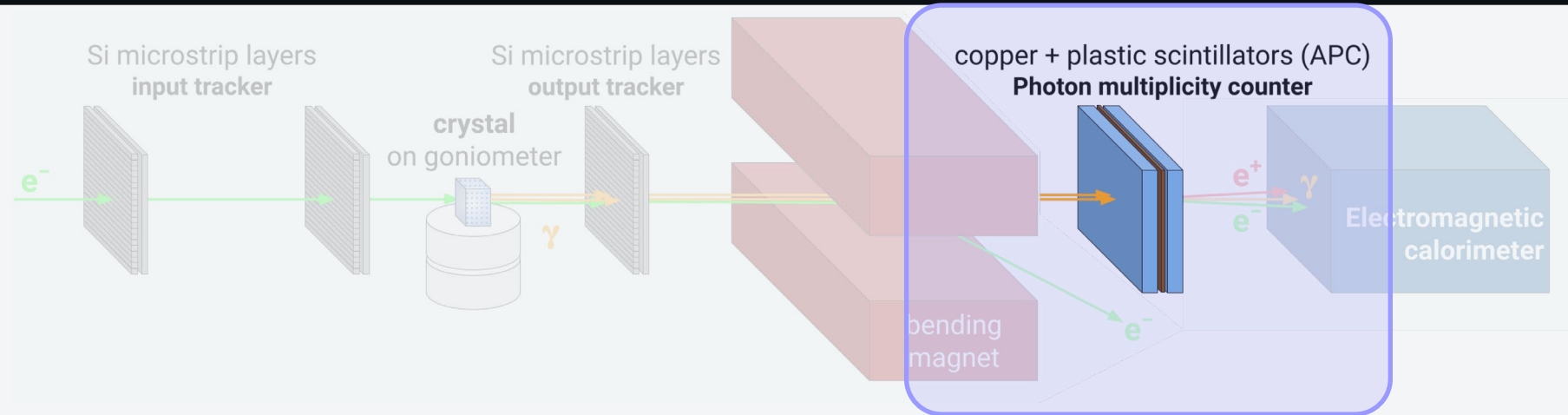


**Magnet**  
Select only the photons

# The setup - output stage

CERN  
configuration

DESY  
configuration

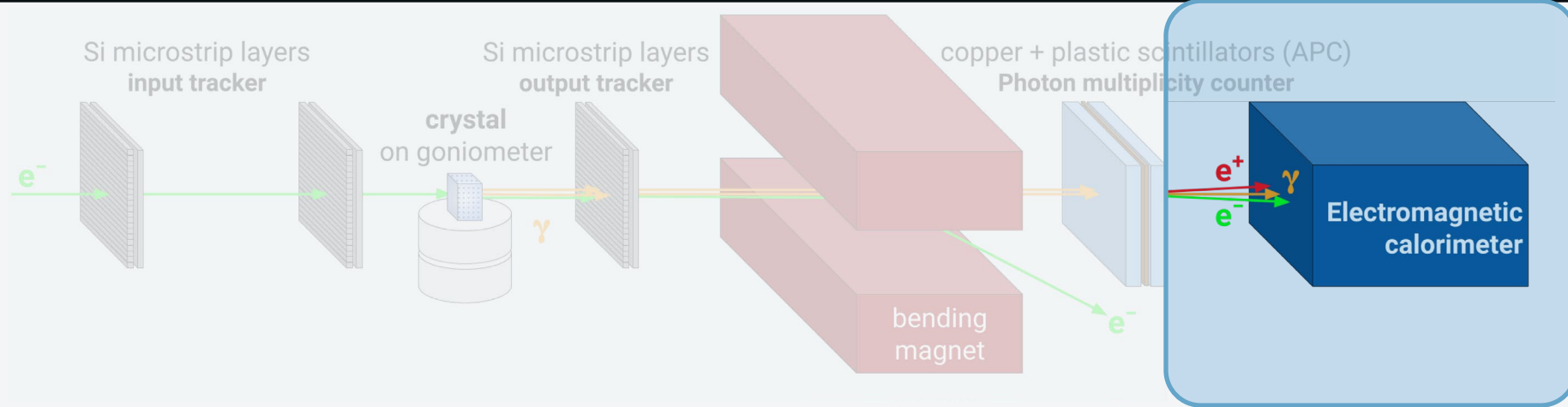


**APC + Cu converter**  
Photon multiplicity counter

# The setup - output stage

CERN  
configuration

DESY  
configuration



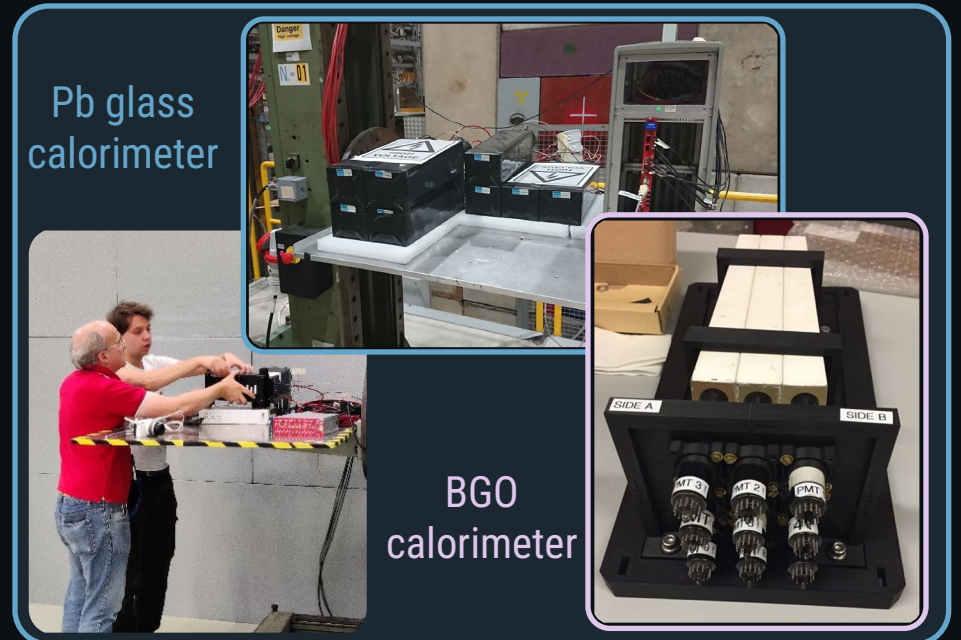
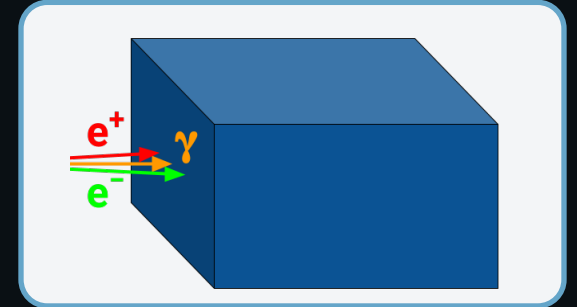
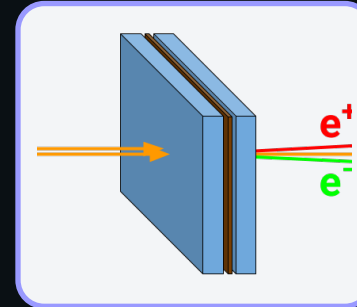
Radiated energy loss  
calorimeter signal

# The setup - output stage

An **Active Photon Converter (APC)** based on plastic scintillators and thin layers of copper ( $0.2X_0$ ) for photo conversion

**Calorimeters** consists in

- $3 \times 3$  matrix of BGO blocks, PMT-based readout
- (OPAL) Lead glass blocks read out by PMTs



Pb glass calorimeter

BGO calorimeter



Active Photon Converter (APC)





# TESTBEAM RESULTS

# DESY T21 line

Electron beams at 5.6 GeV/c



W of 2.25 mm (0.64 X0) aligned along  $\langle 100 \rangle$  axis.

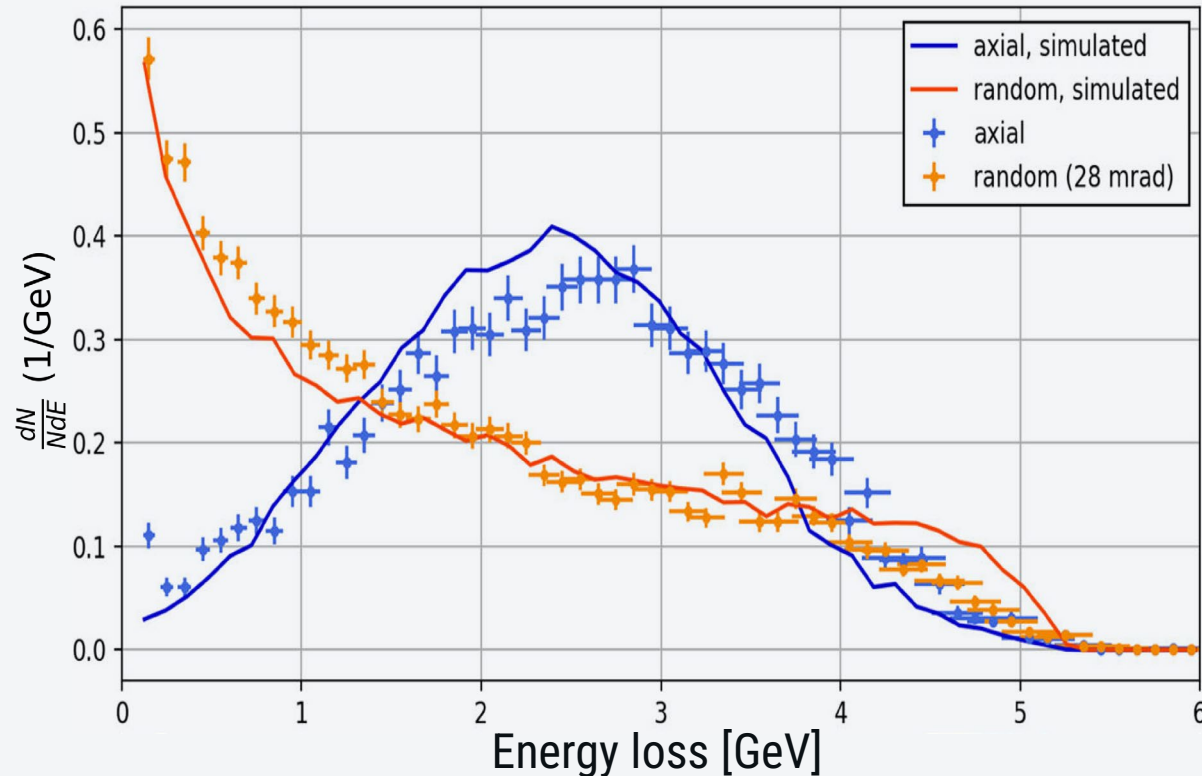
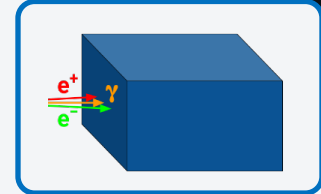
(research center manufactured crystal)

# Radiated energy loss



DESY setup configuration

## Calorimeter Signal – Energy loss of W 2.25mm ( $\sim 0.65X_0$ ) $\langle 001 \rangle$



Clear difference in energy loss distribution.  
In axial orientation : **peaks above 2.5 GeV**,  
In amorphous orientation it **vanishes** as typical for  
Bremsstrahlung

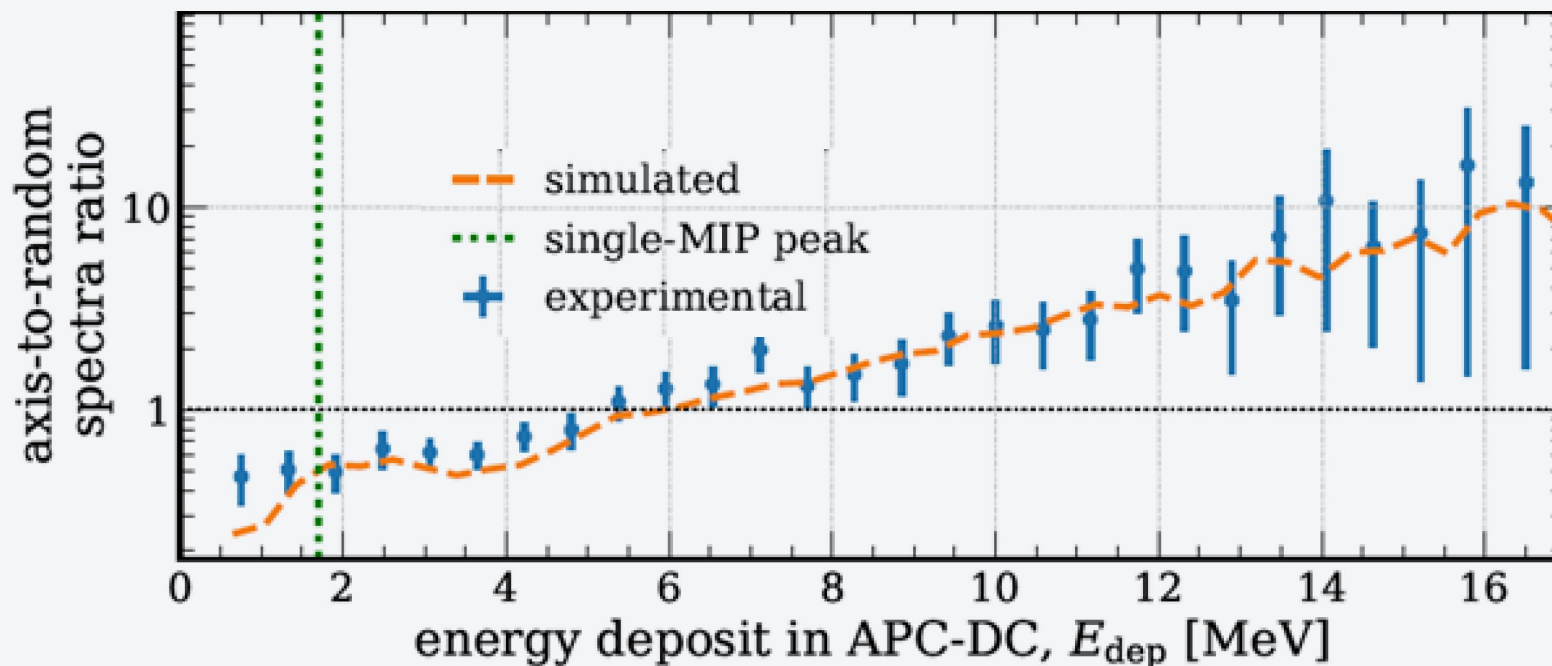
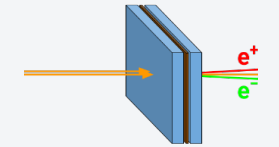
Bandiera et al. [4]

# Active Photon Converter (APC)



DESY setup configuration

Active Photon Converter (Photon multiplicity counter)  
axial to amorphous signal of  $W$  2.25mm ( $\sim 0.65X_0$ )  $\langle 001 \rangle$



Clear enhancement of photon production in axial orientation case

*Bandiera et al. [4]*

# CERN PS

Electron beams at 6 GeV/c



W of 1.5 - 2 mm (0.43 – 0.57  $X_0$ ) aligned along  $\langle 111 \rangle$  axis. (industrial manufactured crystals)

lr of 1 - 2 mm (0.34 – 0.68  $X_0$ ) aligned along  $\langle 110 \rangle$  axis. (industrial manufactured crystals)

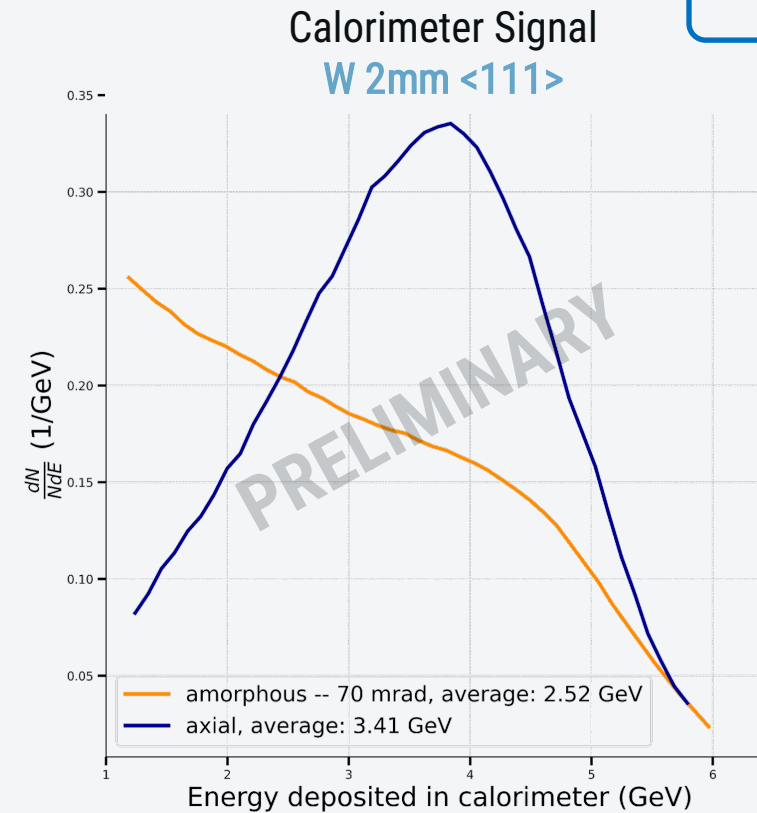
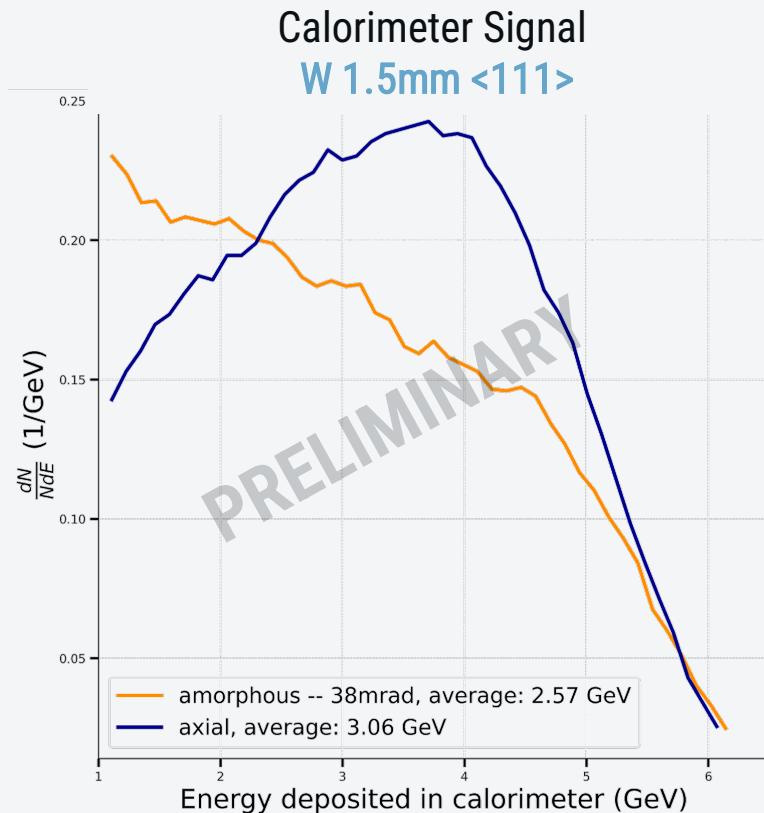
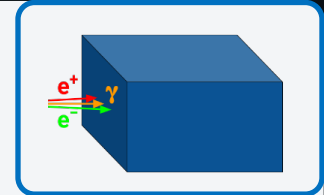


# Radiated energy loss



CERN setup configuration

For both the **W** and **Ir** aligned along the **<111> axes** and the **<110> axes**, respectively, the radiative energy loss distribution peaks above 3.5 GeV, while for amorphous orientation it vanishes as typical for Bremsstrahlung

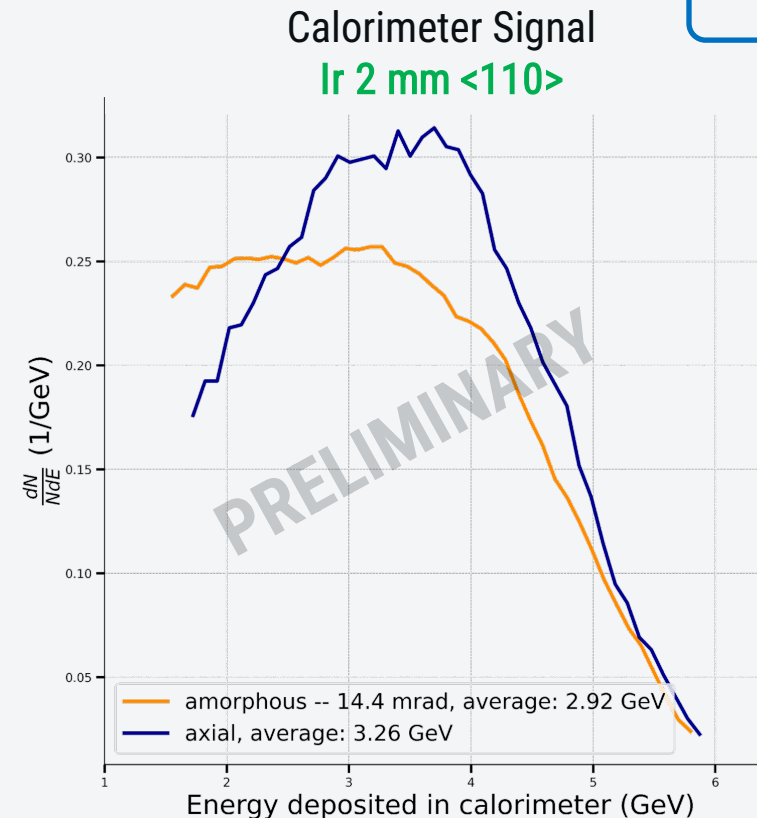
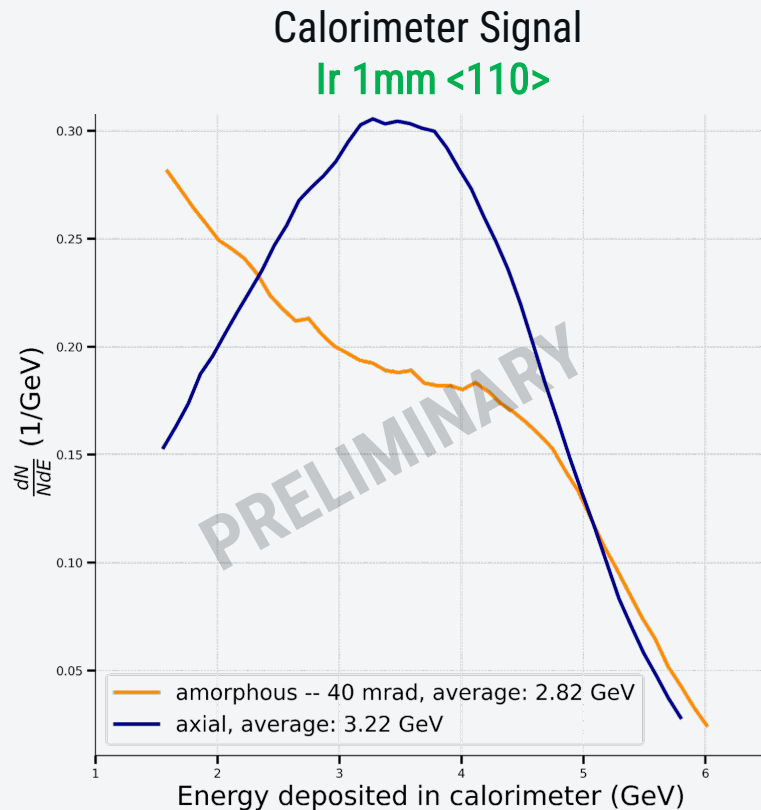
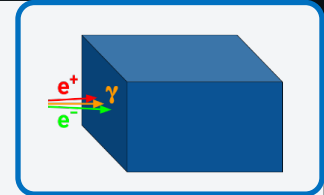


# Radiated energy loss



CERN setup configuration

For both the **W** and **Ir** aligned along the **<111> axes** and the **<110> axes**, respectively, the radiative energy loss distribution peaks above 3.5 GeV, while for amorphous orientation it vanishes as typical for Bremsstrahlung

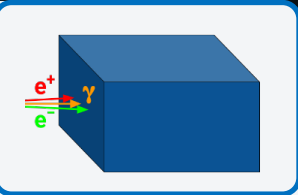


# Radiated energy loss - Transition

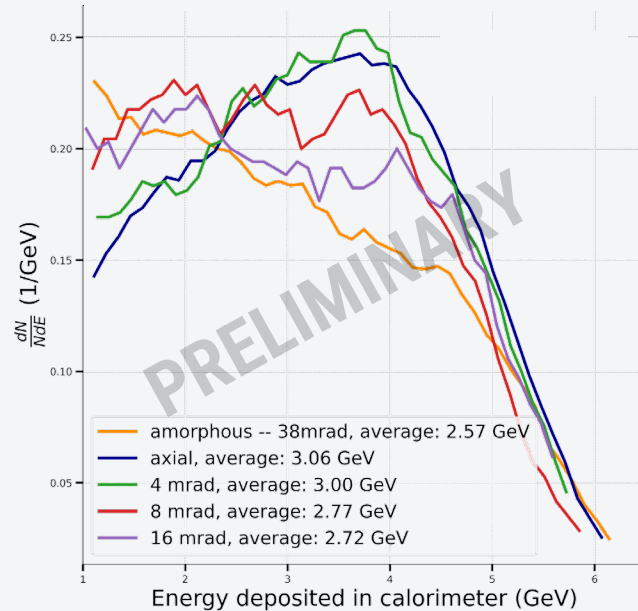


CERN setup configuration

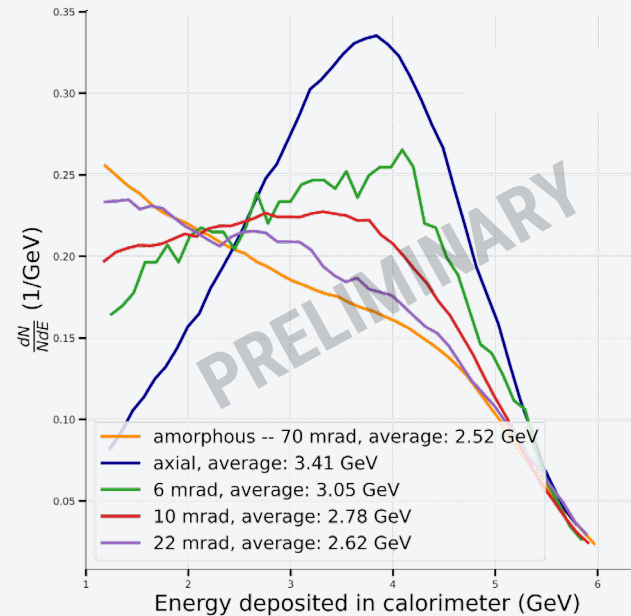
For both the **W** and **Ir** aligned along the **<111> axes** and the **<110> axes**, respectively, the radiative energy loss distribution peaks above 3.5 GeV, while for amorphous orientation it vanishes as typical for Bremsstrahlung



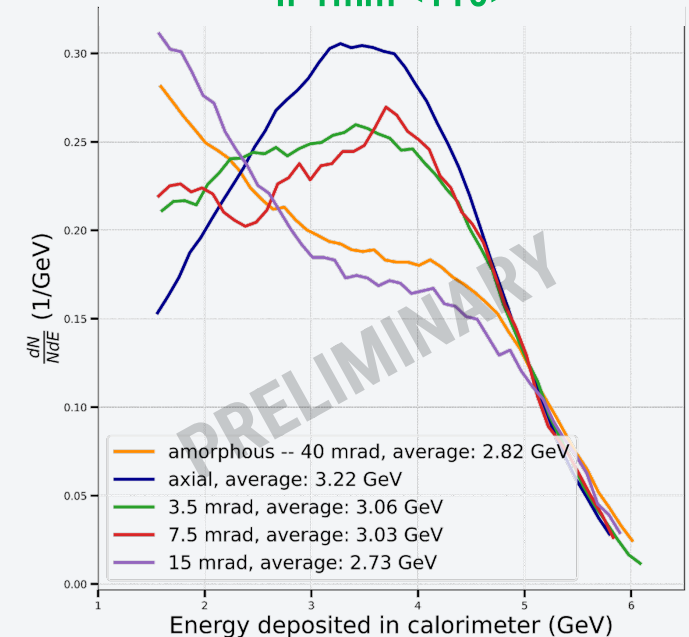
Calorimeter Signal  
**W 1.5mm <111>**



Calorimeter Signal  
**W 2mm <111>**



Calorimeter Signal  
**Ir 1mm <110>**



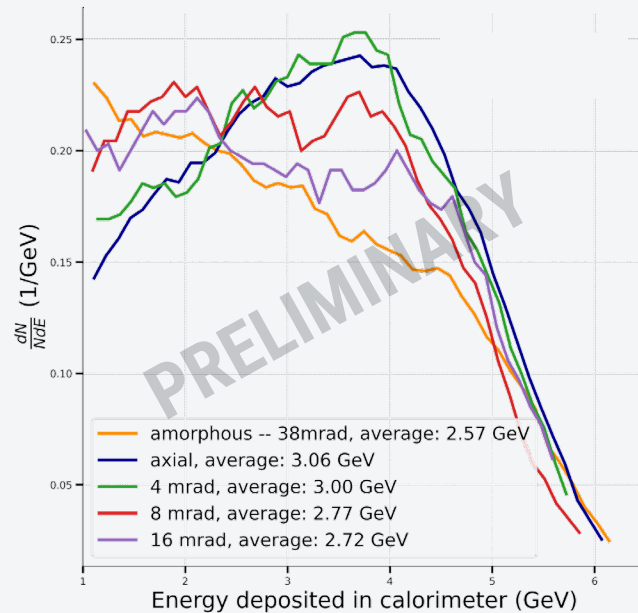
# Radiated energy loss - Transition



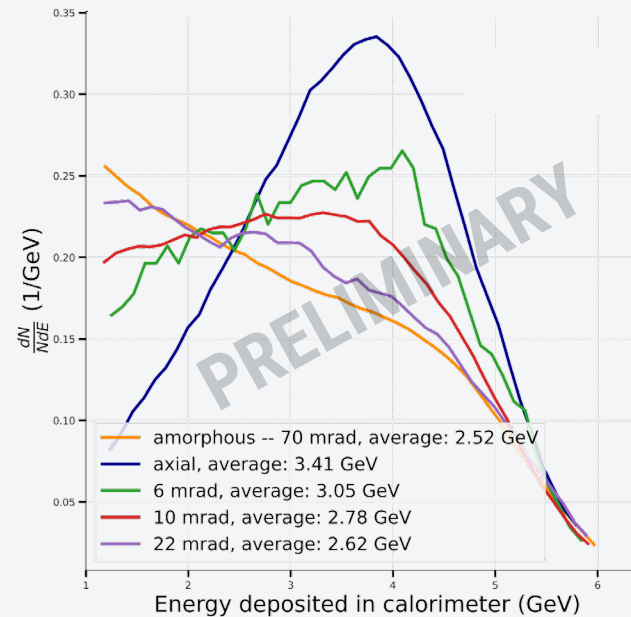
CERN setup configuration

We observed continuous transition from amorphous to aligned mode with the axis, extending 15 mrad, *i.e.* much wider the critical angle ( $\sim 0.6$  mrad).

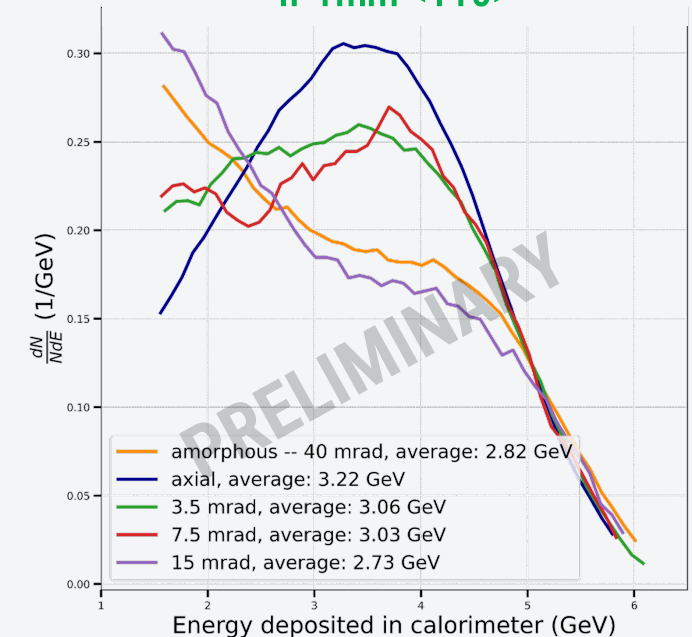
Calorimeter Signal  
W 1.5mm  $\langle 111 \rangle$



Calorimeter Signal  
W 2mm  $\langle 111 \rangle$



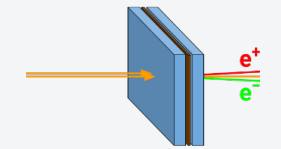
Calorimeter Signal  
Ir 1mm  $\langle 110 \rangle$



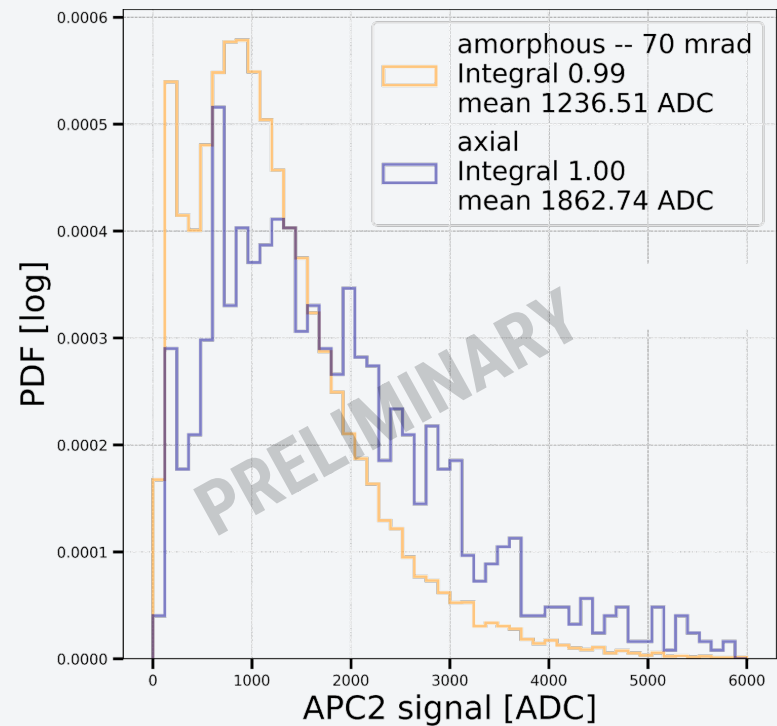
# Active Photon Converter (APC)



CERN setup configuration



APC Signal  
W 2 mm  $\langle 111 \rangle$



Clear enhancement of the energy deposited in the second scintillator, thus **more photon production** in axial orientation case





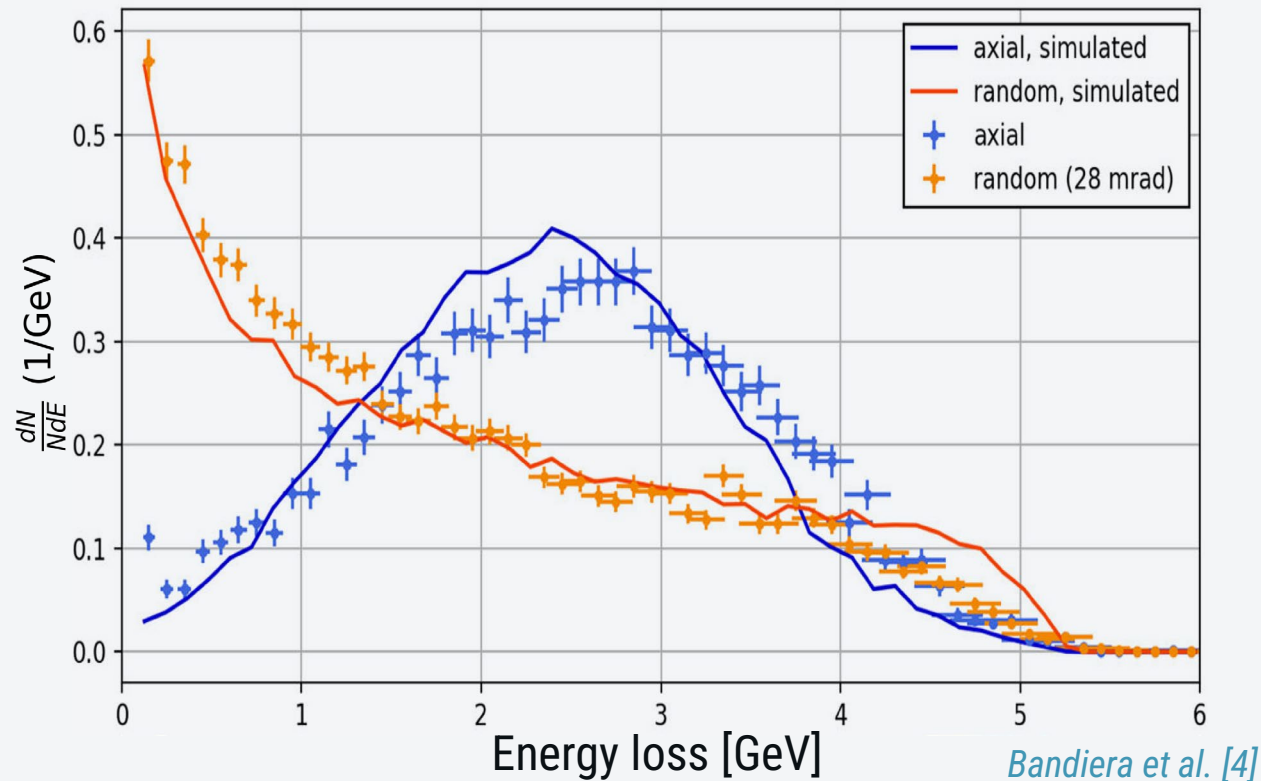
# **SIMULATION CODE VALIDATION**

# Our simulation code WORKS !



DESY setup configuration

## Calorimeter Signal – Energy loss of W 2.25mm ( $\sim 0.65X_0$ ) $\langle 001 \rangle$



The results from beam tests conducted at DESY and CERN PS **agrees** with the Monte Carlo simulation:

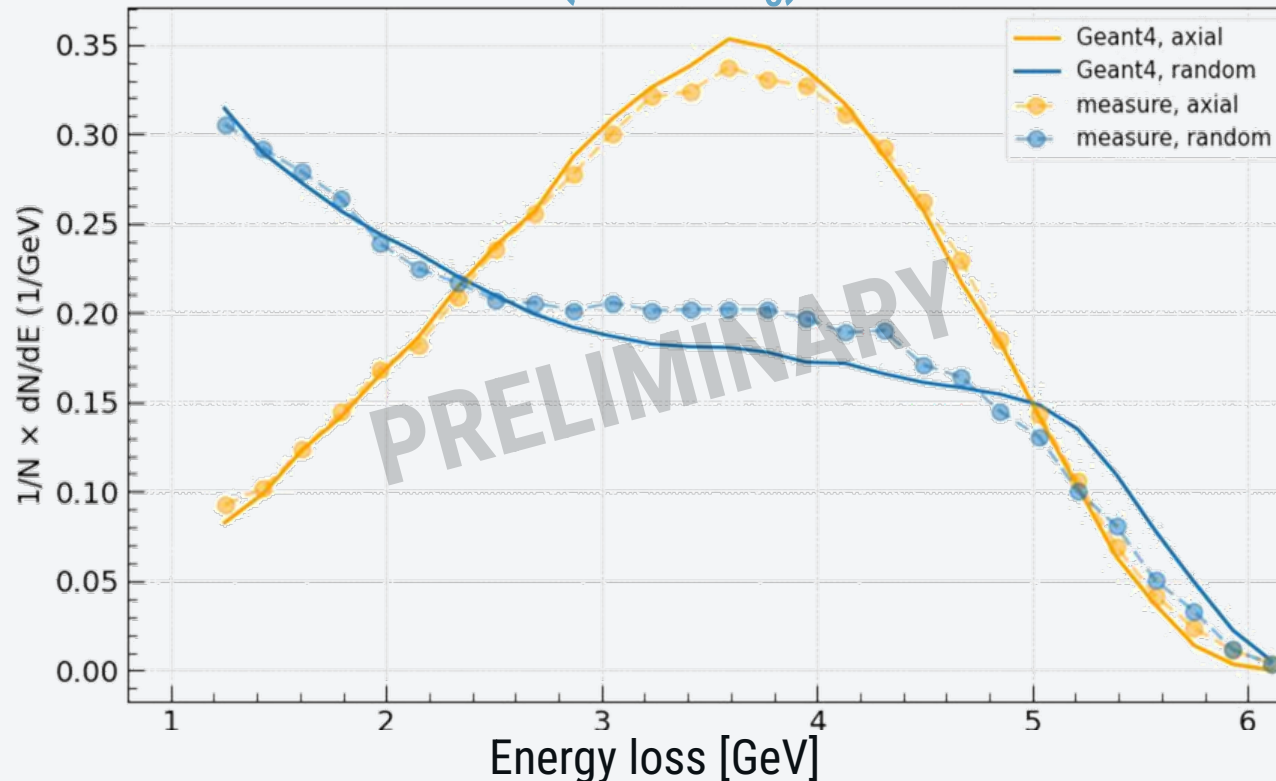
- The whole setup was simulated using the Geant4 toolkit with the new *G4ChannelingFastSim* library  
*A. Sytov et al. [5 – 6]*
- The output file encompassing all secondary  $\gamma$  and  $e^\pm$  particles considers the interactions within the entire experimental setup.  
*Bandiera et al. [4]*

# Our simulation code WORKS !



CERN setup configuration

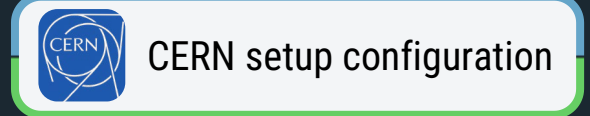
Calorimeter Signal – Energy loss of  
 $W$  2mm ( $\sim 0.57X_0$ )  $\langle 111 \rangle$



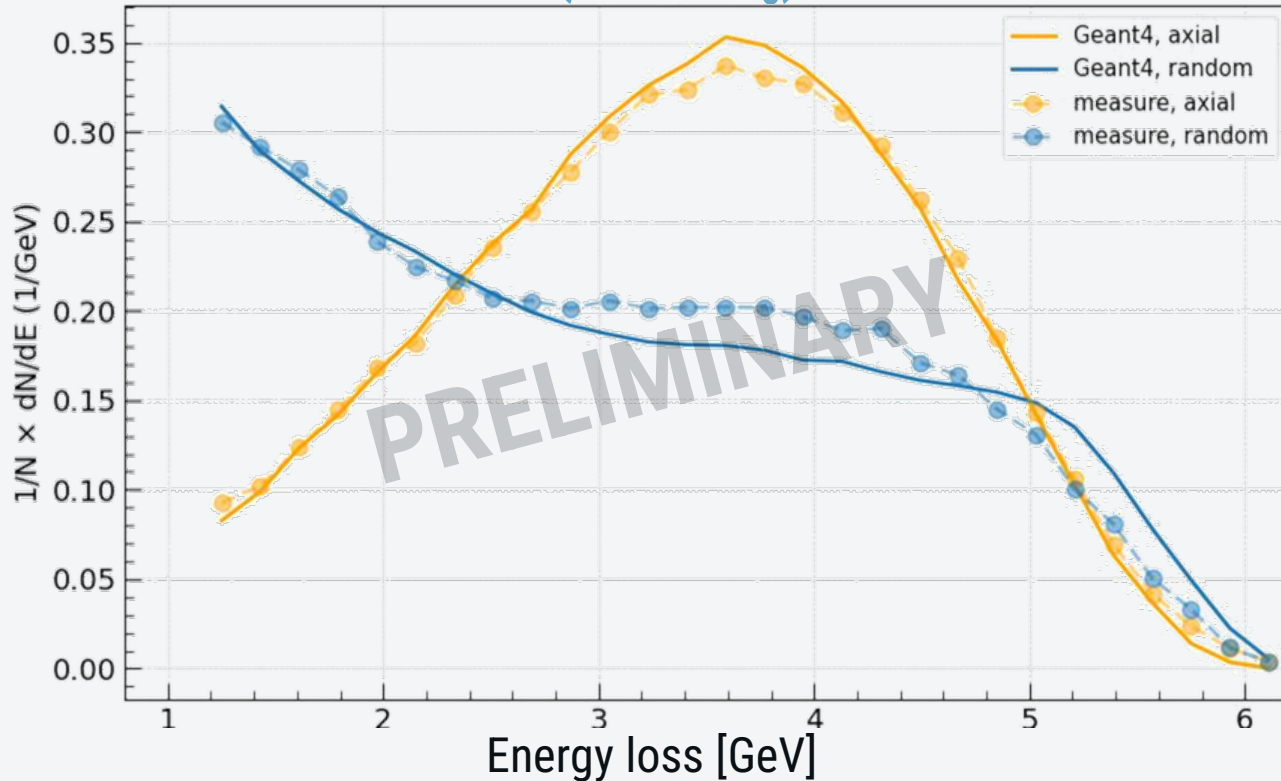
The results from beam tests conducted at DESY and CERN PS **agrees** with the Monte Carlo simulation:

- The whole setup was simulated using the Geant4 toolkit with the new *G4ChannelingFastSim* library  
[A. Sytov et al. \[5 – 6\]](#)
- The output file encompassing all secondary  $\gamma$  and  $e^\pm$  particles considers the interactions within the entire experimental setup.  
[Bandiera et al. \[4\]](#)

# Our simulation code WORKS !



Calorimeter Signal – Energy loss of  
 $W$  2mm ( $\sim 0.57X_0$ )  $\langle 111 \rangle$



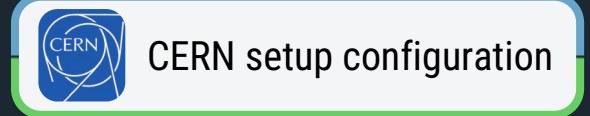
The results from beam tests conducted at DESY and CERN PS **agrees** with the Monte Carlo simulation:

- The whole setup was simulated using the Geant4 toolkit with the new *G4ChannelingFastSim* library  
[A. Sytov et al. \[5 – 6\]](#)
- The output file encompassing all secondary  $\gamma$  and  $e^\pm$  particles considers the interactions within the entire experimental setup.  
[Bandiera et al. \[4\]](#)

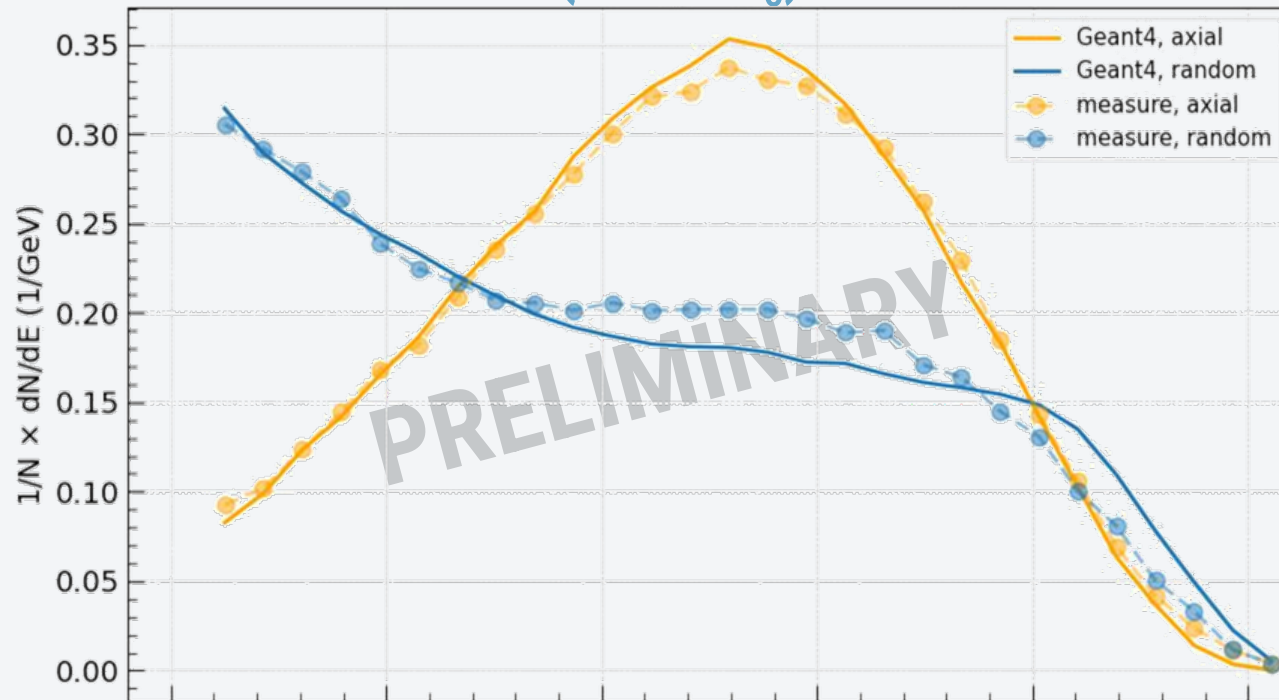
Once the simulation environment was validated against experimental findings, efforts were directed towards optimizing the FCC-ee positron source scheme.

Parameters chosen for the FCC-ee positron source optimization via Geant4

# Our simulation code WORKS !



Calorimeter Signal – Energy loss of  
 $W$  2mm ( $\sim 0.57X_0$ )  $\langle 111 \rangle$



As seen in A. Sytov and G.Paternò talks of 05/11/2024

The results from beam tests conducted at DESY and CERN PS agrees with the Monte Carlo simulation:

- The whole setup was simulated using the Geant4 toolkit with the new *G4ChannelingFastSim* library  
*A. Sytov et al. [5 – 6]*
- The output file encompassing all secondary  $\gamma$  and  $e^\pm$  particles considers the interactions within the entire experimental setup.  
*Bandiera et al. [4]*

Once the simulation environment was validated against experimental findings, efforts were directed towards optimizing the FCC-ee positron source scheme.

Parameters chosen for the FCC-ee positron source optimization via Geant4



A dark, futuristic perspective of a carbon nanotube structure. The tube is composed of a lattice of dark spheres (atoms) connected by thin rods (bonds). The structure is illuminated from the right, creating a bright, glowing light source at the end of the tube. The background is dark with some faint, out-of-focus light spots.

**FUTURE  
PERSPECTIVE**

# Future Perspective

- Comparison with simulations:
  - W 1.5 mm
  - Ir
- Optimization of the hybrid source for 2.86 GeV/c

- Future test at CERN PS
  - New energy baseline ( $e^-$  2.86 GeV/c )
  - Single crystal

# Future Perspective

- Comparison with simulations:
  - W 1.5 mm
  - Ir
- Optimization of the hybrid source for 2.86 GeV/c

- Future test at CERN PS
  - New energy baseline ( $e^-$  2.86 GeV/c )
  - Single crystal

Optimization of hybrid and single crystal including test of radiator converter for CHART P3 project







Further contact:

Laura Bandiera (INFN-Ferrara)  
[bandiera@fe.infn.it](mailto:bandiera@fe.infn.it)



[ncanale@fe.infn.it](mailto:ncanale@fe.infn.it)

Iryna Chaikovska (IJCLab)  
[iryna.chaikovska@ijclab.in2p3.fr](mailto:iryna.chaikovska@ijclab.in2p3.fr)

# References and Acknowledgment

## References:

- [1] Frank Zimmermann, FCC Week 2024 10-14 June
- [2] R. Chehab et al., NIM B 266 (2008)
- [3] X. Artru, I. Chaikovska, R. Chehab et al. NIM B 355 (2015)
- [4] L. Bandiera et al., Eur. Phys. J. C 82 (2022)
- [5] A. Sytov et al. Phys. Rev. Accel. Beams 22 (2019)
- [6] A. Sytov et al. JKPS 83 (2023)

## Acknowledgement:

We acknowledge financial support under the National Recovery and Resilience Plan (NRRP), Call for tender No. 104 published on 02.02.2022 by the Italian Ministry of University and Research (MUR), funded by the European Union – NextGenerationEU – Project Title : "*Intense positron source Based On Oriented crySTals - e+BOOST*" 2022Y87K7X – CUP I53D23001510006







**BACKUP**



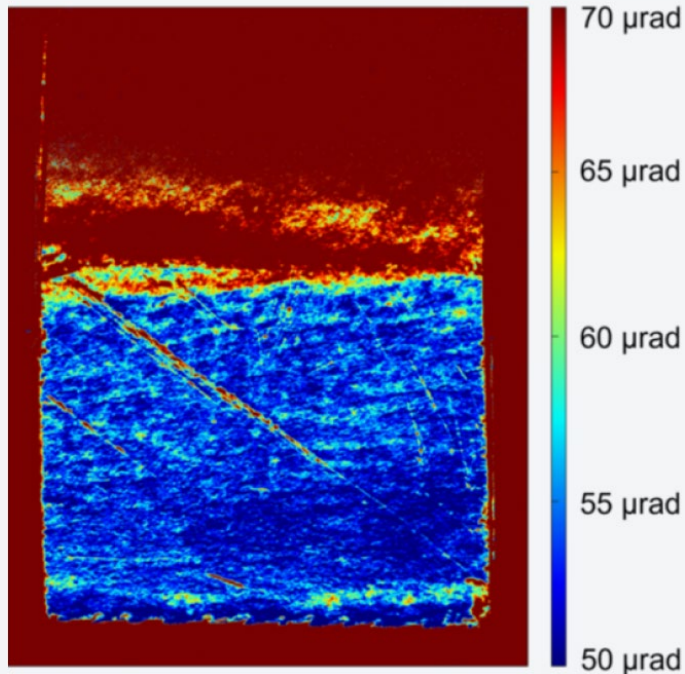


# CRYSTAL CHARACTERIZATION

# Research center crystals quality check



W 2.25mm  
( $\sim 0.65X_0$ )  
<001>



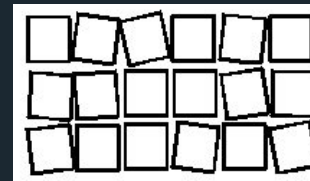
Imaging of the sample mosaicity measured at BM05 beamline of ESRF.

Color indicates the mosaicity of the sample

Characterization of mosaicity of the lattice performed at ESR Synchrotron (Grenoble, France) (20 keV X rays)

Mosaicity  $\leq 60 \mu\text{rad}$ .

largest mosaicity are still below  $150 \mu\text{rad}$  near the scratches

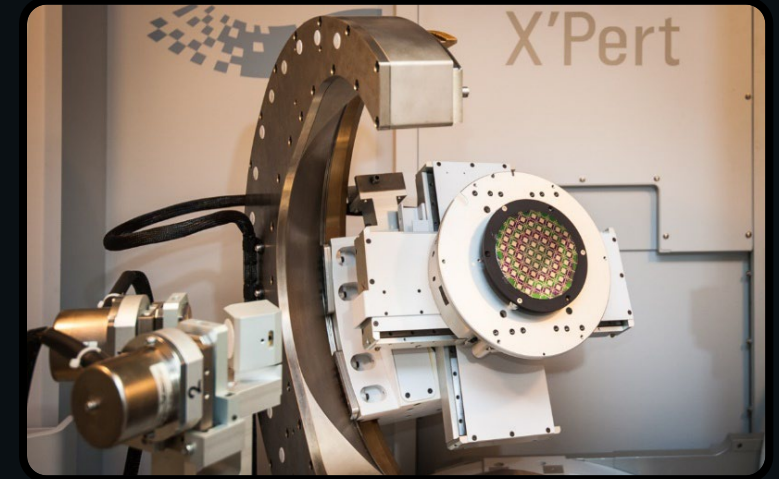


*In crystallography, the **mosaicity** is a measure of the spread of crystal plane orientations*

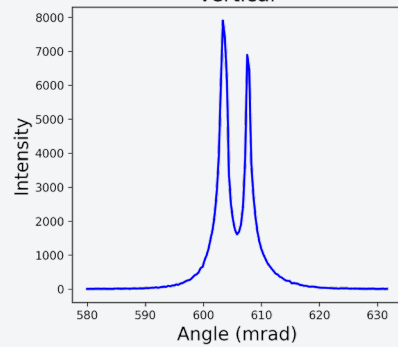
# Industrial crystals quality check



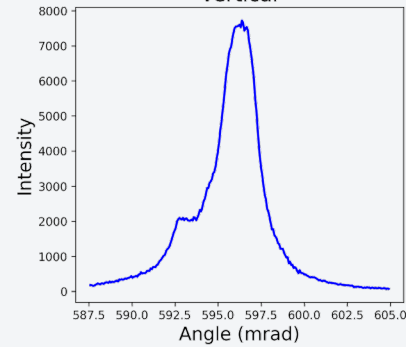
Characterization of superficial mosaicity of the lattice performed with High Resolution XRD at laboratories of Ferrara (@ 8.04 keV)



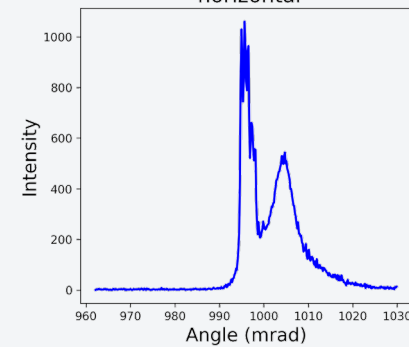
**Ir <110> 1 mm**  
vertical



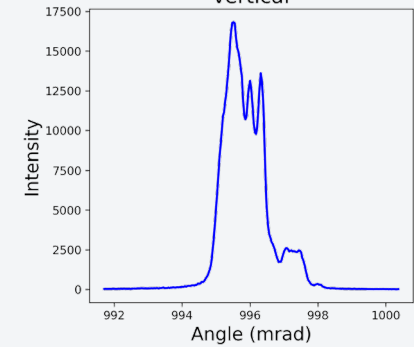
**Ir <110> 2 mm**  
vertical



**W <111> 1.5 mm (1)**  
horizontal



**W <111> 2 mm**  
vertical

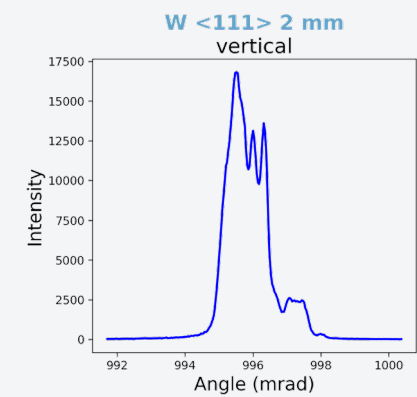
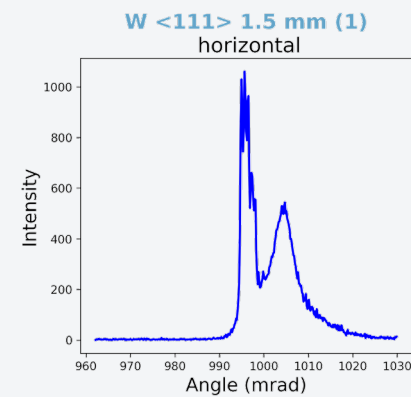
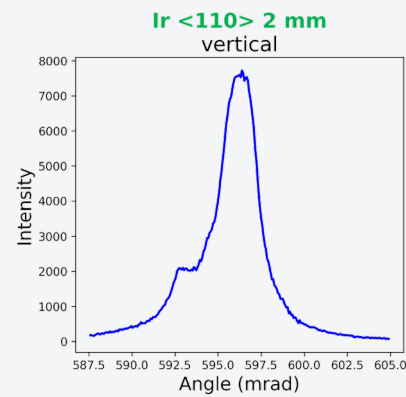
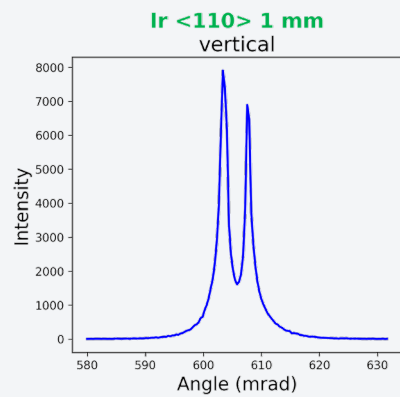
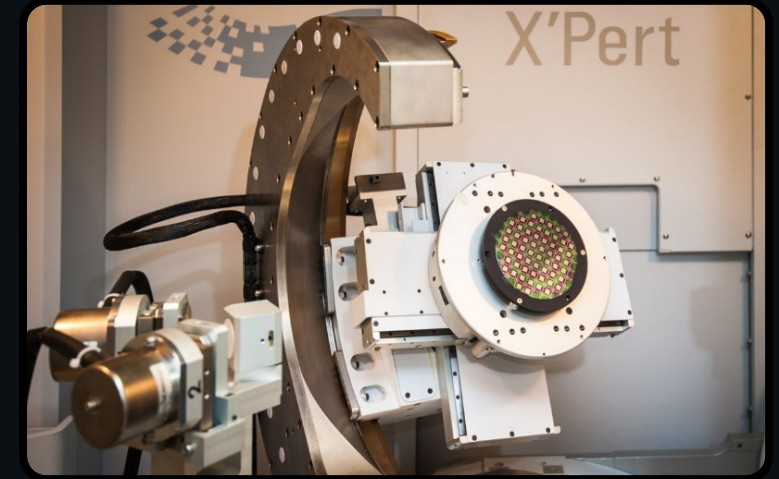


# Industrial crystals quality check

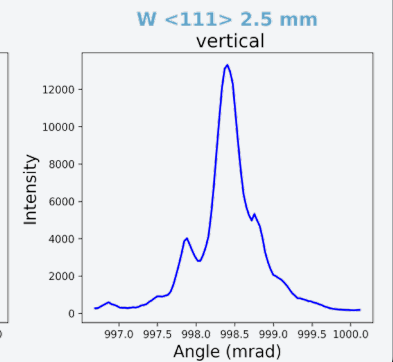
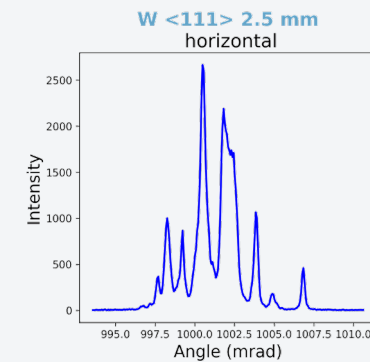
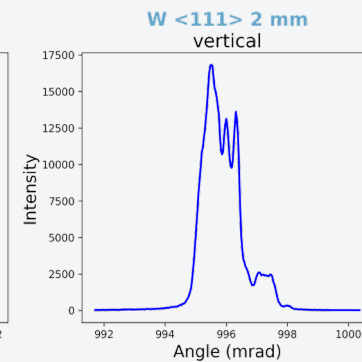
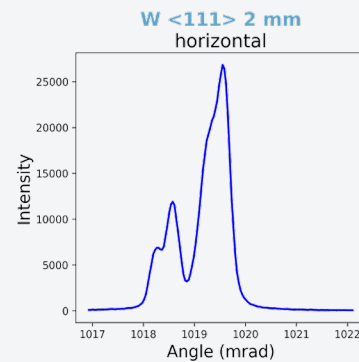
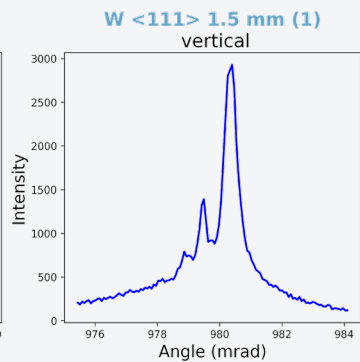
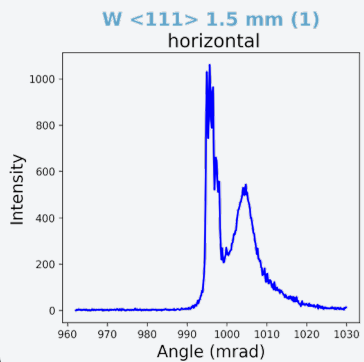
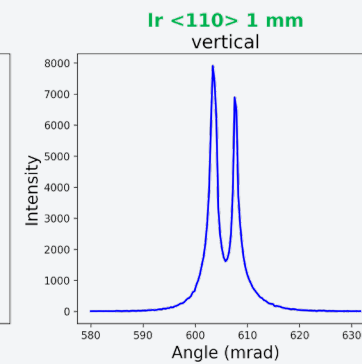
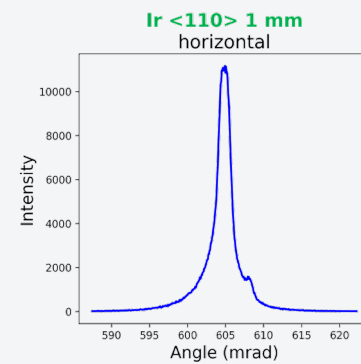
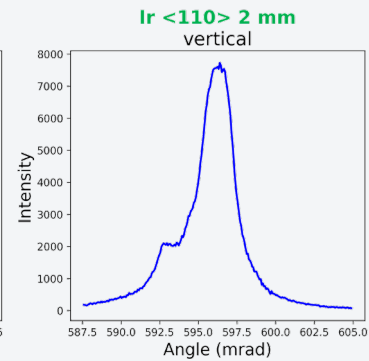
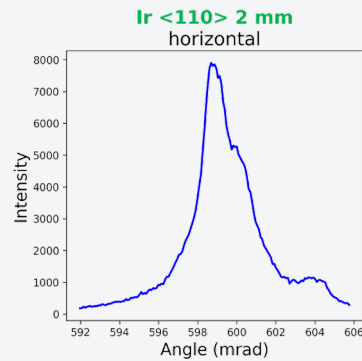


Characterization of superficial mosaicity of the lattice performed with High Resolution XRD at laboratories of Ferrara (@ 8.04 keV)

FWHM of industrial crystal is wider than the critical angle, the coherent effects are still available?



# Summary of HRXRD test for CERN samples



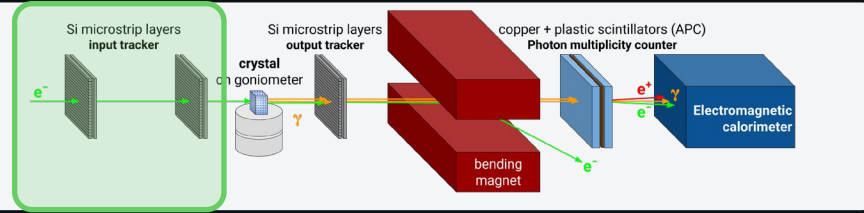




# INPUT TRACKERS

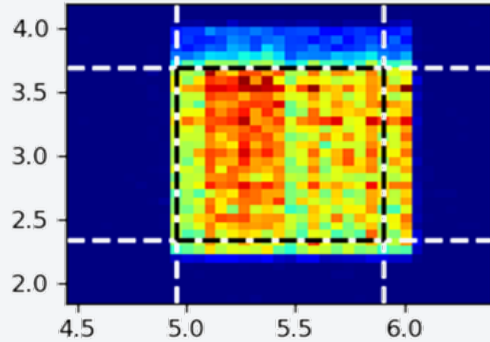


# The setup

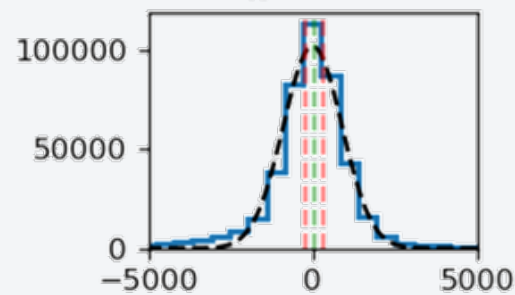


**Input stage**  
Reconstruct track and  
impinging angle on the crystal

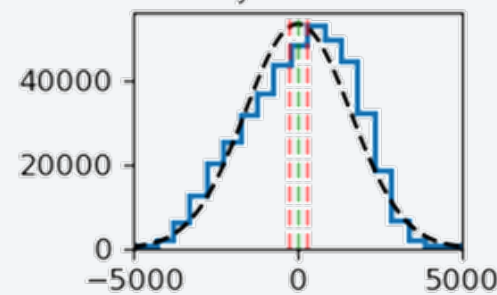
Chamber 2 position map



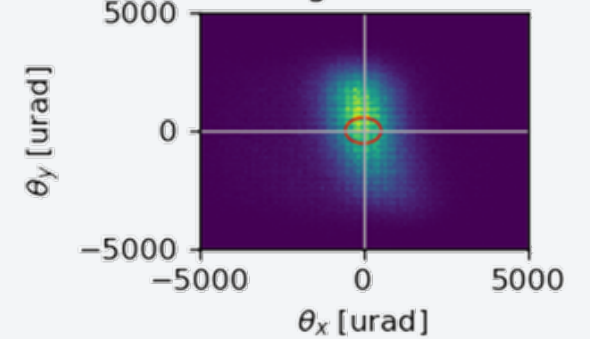
$\theta_{x \text{ in axial}}$



$\theta_{y \text{ in axial}}$



divergence axial

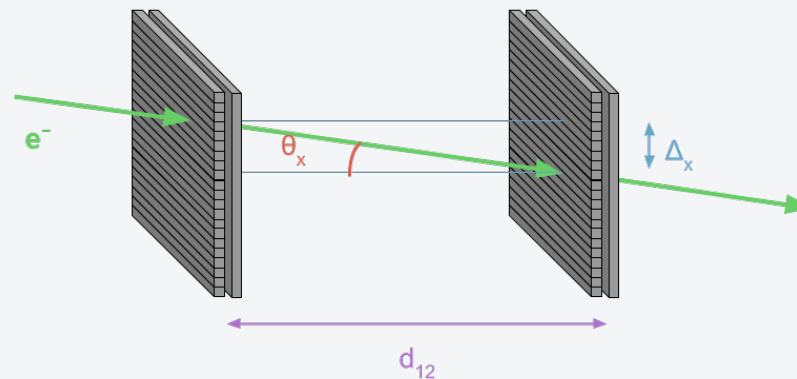


## Hit position on Chamber weighted by Calo signal

### input tracker

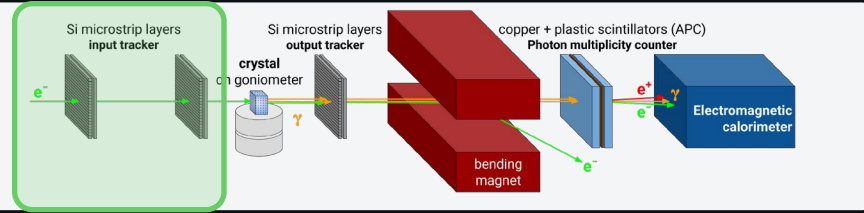
$\sim 2 \times 2$  or  $9.5 \times 9.5 \text{ cm}^2$  xy double-sided Si microstrip sensors, with an overall  $\sim 10 \mu\text{m}$  single-hit resolution self-triggering on strip to select the proper area

## $\vartheta_{IN}$ reconstructed at crystal entrance



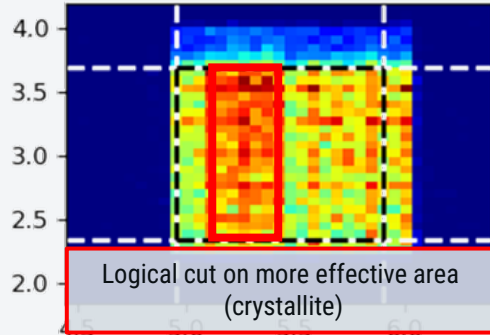
$$\vartheta_x = \arctan(\Delta_x / d_{12})$$

# The setup

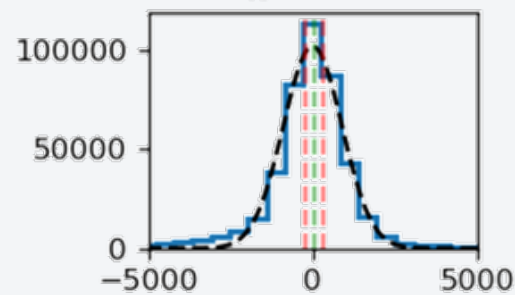


**Input stage**  
Reconstruct track and  
impinging angle on the crystal

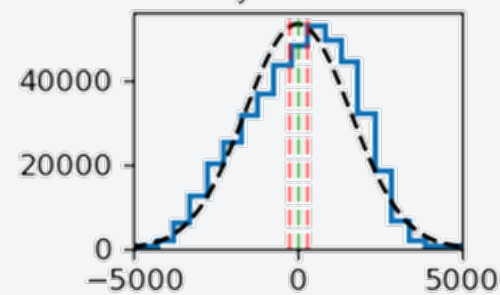
Chamber 2 position map



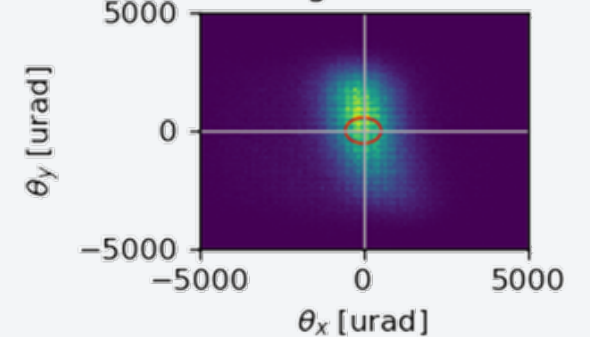
$\theta_{x \text{ in axial}}$



$\theta_{y \text{ in axial}}$



divergence axial

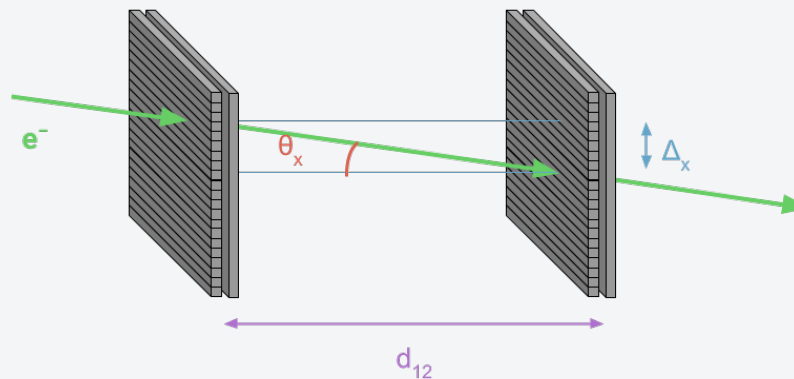


## Hit position on Chamber weighted by Calo signal

### input tracker

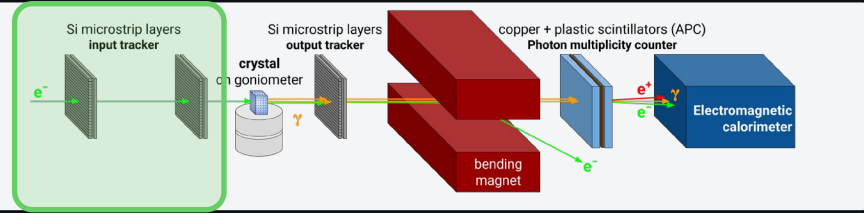
$\sim 2 \times 2$  or  $9.5 \times 9.5 \text{ cm}^2$  xy double-sided Si microstrip sensors, with an overall  $\sim 10 \mu\text{m}$  single-hit resolution self-triggering on strip to select the proper area

## $\vartheta_{IN}$ reconstructed at crystal entrance



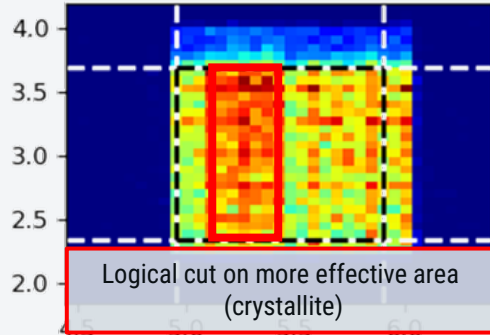
$$\vartheta_x = \arctan(\Delta_x / d_{12})$$

# The setup

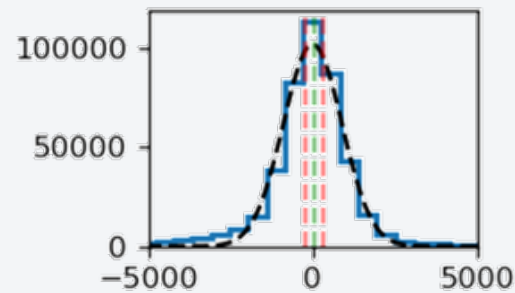


**Input stage**  
Reconstruct track and  
impinging angle on the crystal

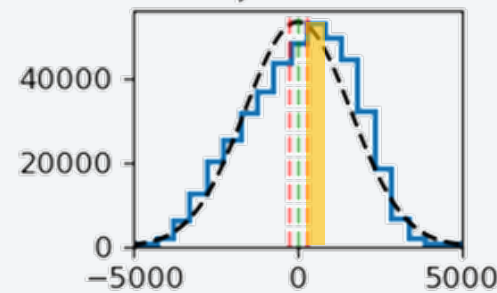
Chamber 2 position map



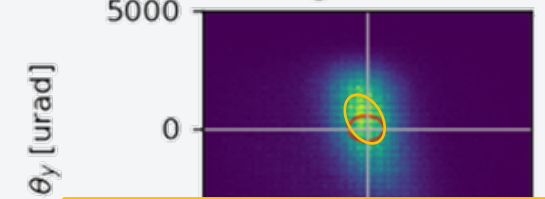
$\theta_{x \text{ in axial}}$



$\theta_{y \text{ in axial}}$



divergence axial



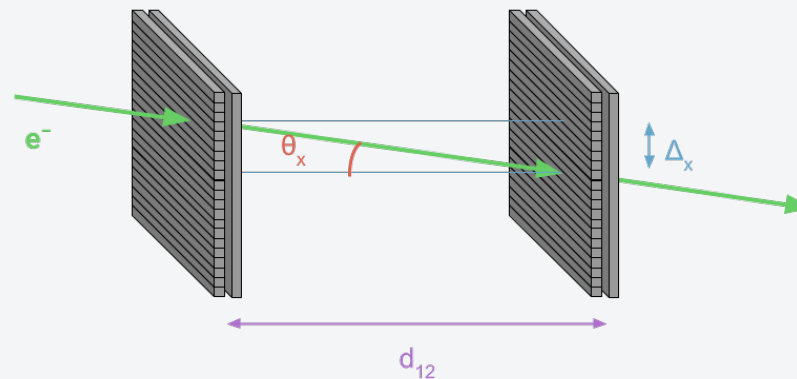
Slightly improvable with  
an elliptic cut on the angle

## Hit position on Chamber weighted by Calo signal

### input tracker

$\sim 2 \times 2$  or  $9.5 \times 9.5$  cm<sup>2</sup> xy double-sided Si microstrip sensors, with an overall  $\sim 10$   $\mu$ m single-hit resolution self-triggering on strip to select the proper area

## $\vartheta_{IN}$ reconstructed at crystal entrance

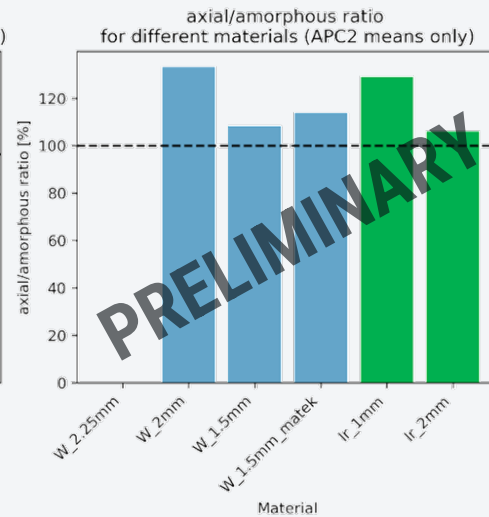
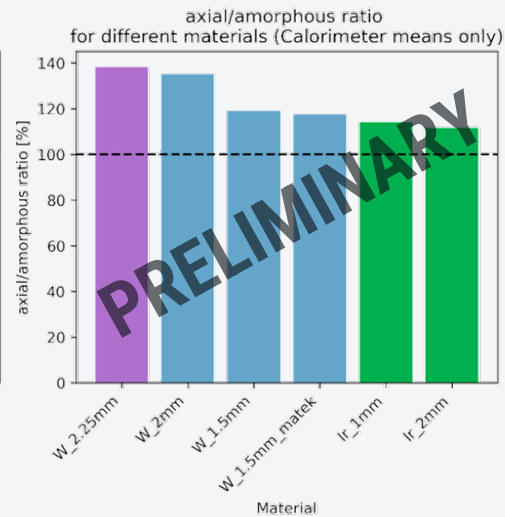
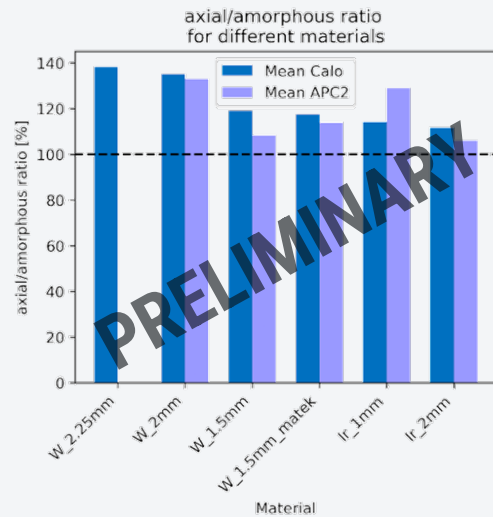


$$\vartheta_x = \arctan(\Delta_x / d_{12})$$



# RESULTS SUMMARY

# Summary



Material	Axial/amorph Calo	Axial/amorph APC2
Ir_1mm <110>	~114 %	~129 %
Ir_2mm <110>	~112 %	~106 %
W_1.5 mm <111>	~119 %	~108 %
W_2mm <111>	~135 %	~133 %
W_2.25 <100>	~138 %	Not calculated





**CONVENTIONAL**  
 **$e^+$  SOURCE PROBLEMS**



# Conventional scheme limitations

As seen  
in A.Sytov and  
G.Paternò talks

## Conventional scheme



# Conventional scheme limitations

As seen  
in A.Sytov and  
G.Paternò talks

## Conventional scheme



## Current (Limited by the target)

- Average energy deposition  
→ target heating/melting
- Peak Energy Deposition Density (PEDD)  
→ Inhomogeneous and instantaneous energy deposition, that cause thermomechanical stresses due to temperature gradient

# Conventional scheme limitations

As seen  
in A.Sytov and  
G.Paternò talks

## Conventional scheme



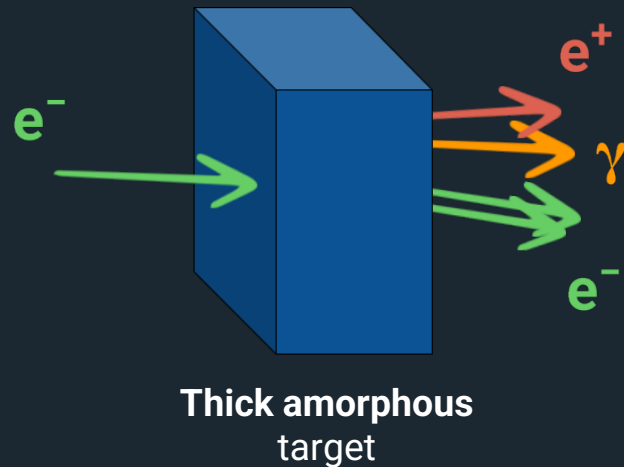
**Current** (Limited by the target)

- Average energy deposition  
→ target heating/melting

# Conventional scheme limitations

As seen  
in A.Sytov and  
G.Paternò talks

## Conventional scheme



## Current (Limited by the target)

- Average energy deposition  
→ target heating/melting
- Peak Energy Deposition Density (PEDD)  
→ Inhomogeneous and instantaneous energy deposition, that cause thermomechanical stresses due to temperature gradient

$e^+$  source set a critical constraint for the peak and average current → Luminosity Constraint!  
Especially for future Linacs

# Hybrid crystal based positron source for $e^-e^+$ colliders

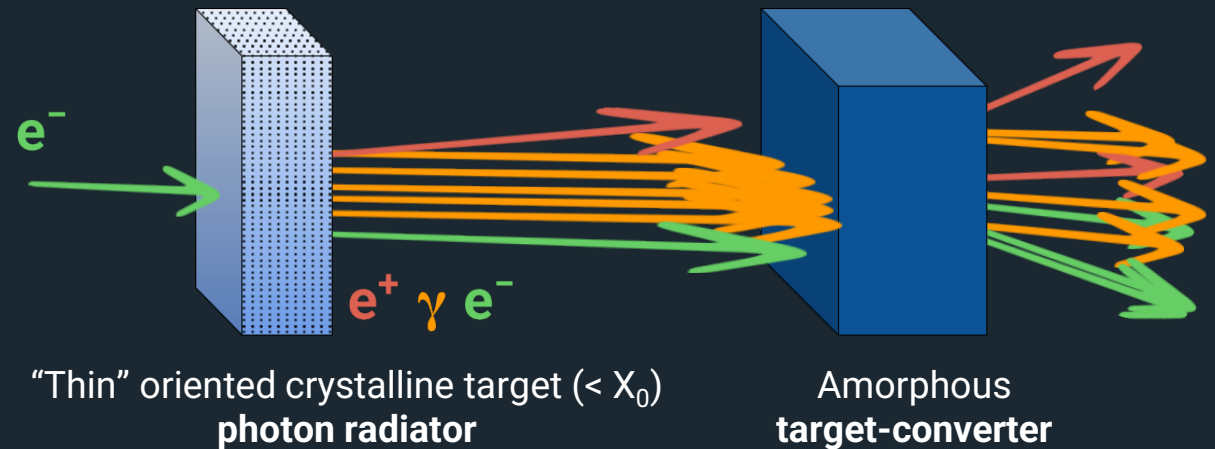
Idea of R. Chehab, A. Variola, V. Strakhovenko and X. Artru [2]

## Conventional scheme



Problem in future Linacs

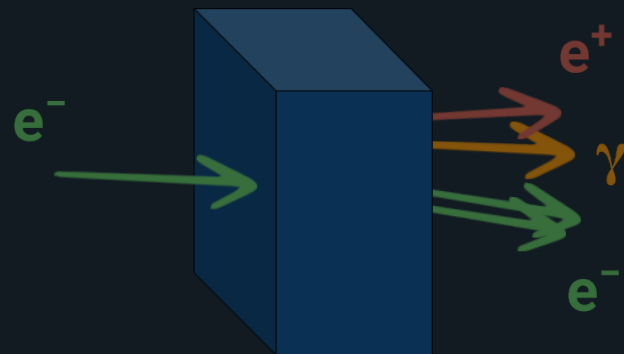
## Hybrid positron source



# Hybrid crystal based positron source for $e^-e^+$ colliders

Idea of R. Chehab, A. Variola, V. Strakhovenko and X. Artru [2]

## Conventional scheme



Thick amorphous target

Problem in future Linacs

## Hybrid positron source



"Thin" oriented crystalline target ( $< X_0$ )  
photon radiator

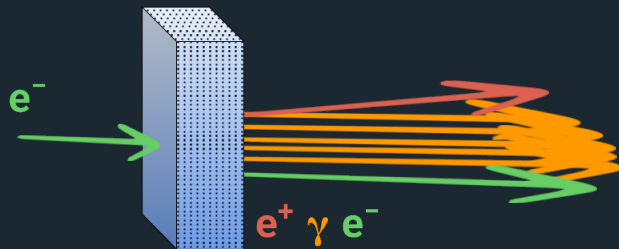
Amorphous target-converter

"Thin" crystal radiator, with thickness  $< X_0$  will limit the heating, enhance the radiation and thus increase the target reliability



# Coherent effects for crystal-based positron sources

## Crystalline photon radiator



"Thin" oriented crystalline target ( $< X_0$ )  
photon radiator

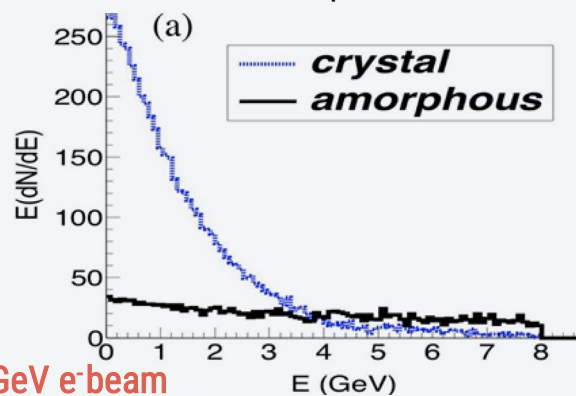
## Hybrid positron source



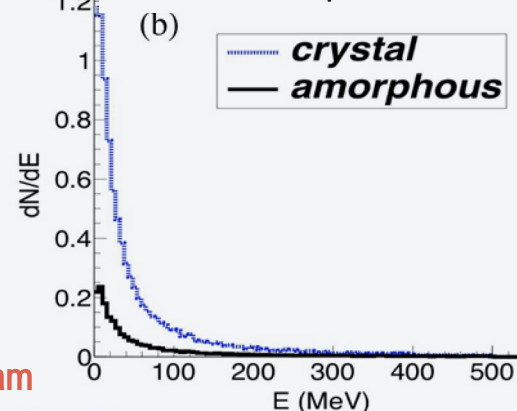
"Thin" crystal ( $< X_0$ )  
photon radiator  
Amorphous  
target-converter

1. Enhancement of photon generation in crystals in coherent conditions  $\rightarrow$  enhancement of pair production in the converter target

## Photon spectrum X. Artru et al. [3]

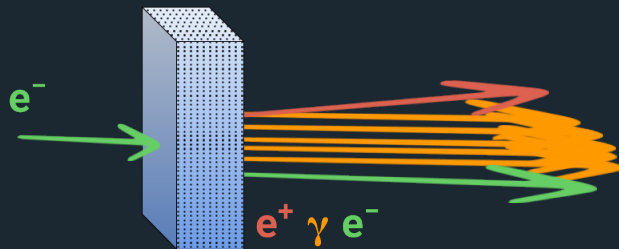


## Positron spectrum X. Artru et al. [3]



# Coherent effects for crystal-based positron sources

## Crystalline photon radiator



"Thin" oriented crystalline target ( $< X_0$ )  
photon radiator

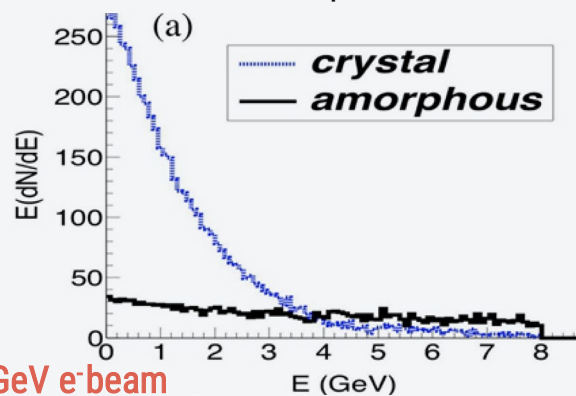
## Hybrid positron source



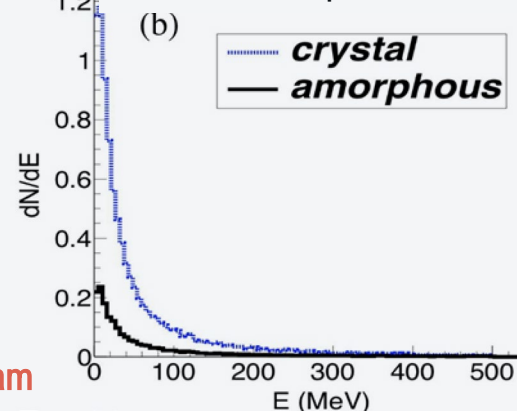
"Thin" crystal ( $< X_0$ )  
photon radiator  
Amorphous  
target-converter

1. Enhancement of photon generation in crystals in coherent conditions  $\rightarrow$  enhancement of pair production in the converter target
2. High rate of soft photons  $\rightarrow$  creation of soft  $e^+$  easily captured in matching systems

### Photon spectrum X. Artru et al. [4]

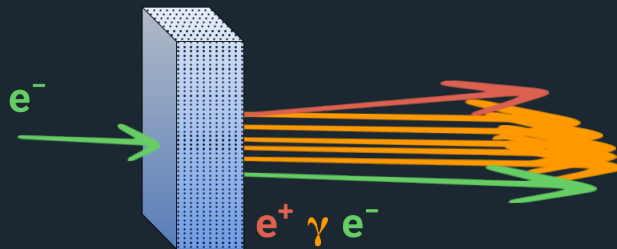


### Positron spectrum X. Artru et al. [4]



# Coherent effects for crystal-based positron sources

## Crystalline photon radiator



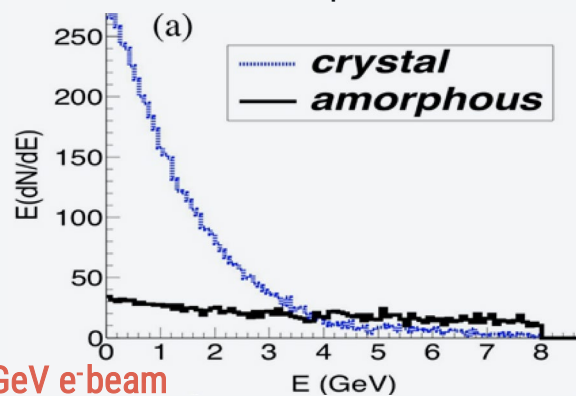
"Thin" oriented crystalline target ( $< X_0$ )  
photon radiator

## Hybrid positron source

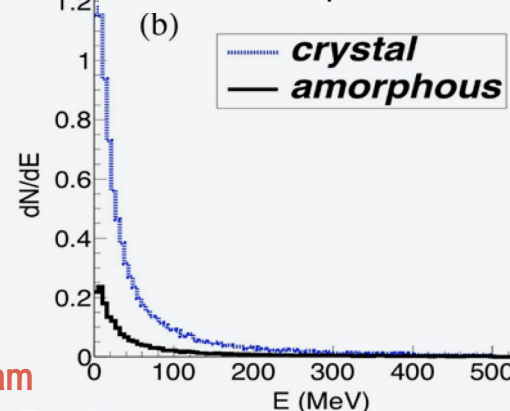


"Thin" crystal ( $< X_0$ )  
photon radiator  
Amorphous  
target-converter

Photon spectrum *X. Artru et al. [3]*



Positron spectrum *X. Artru et al. [3]*

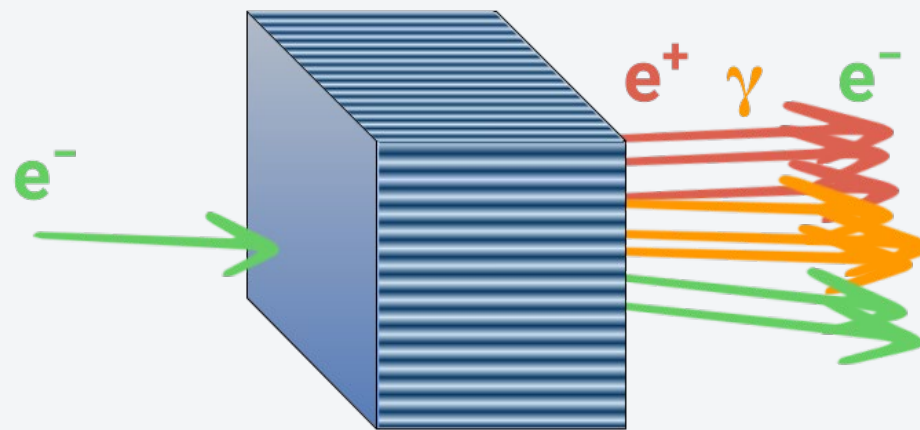


1. Enhancement of photon generation in crystals in coherent conditions → enhancement of pair production in the converter target
2. High rate of soft photons → creation of soft e<sup>+</sup> easily captured in matching systems
3. **Decrease of the PEDD** in the converter

*Bandiera et al. [4]*

# Coherent effects for crystal-based positron sources

## Or a Single Thick Crystal



The performances are very similar to the hybrid source.

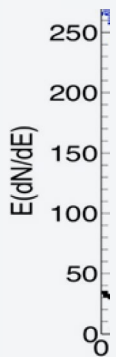
We can use just one device to optimize the positron source of FCC-ee

As seen  
in G.Paternò talk

Crystal

$e^-$

"Thin"



8 GeV  $e^-b\bar{e}$

enhancement of  
photon generation in  
crystals in coherent  
conditions  $\rightarrow$   
enhancement of pair  
production in the  
converter target

increase of the PEDD  
the converter

*Bandiera et al. [4]*